

國立臺灣大學醫學院分子醫學研究所

碩士論文

Graduate Institute of Molecular Medicine

College of Medicine

National Taiwan University

Master Thesis

Rab11 在果蠅神經元樹突修剪所扮演之角色

The role of Rab11 GTPase in neuronal pruning of

Drosophila sensory neurons

高皓翔

Hao-Hsiang Kao

指導教授：李秀香 博士

Advisor: Hsiu-Hsiang Lee, Ph.D.

中華民國 108 年 8 月

August 2019



誌謝



首先要感謝我的指導教授李秀香老師花費了非常多心力指導我寫作此篇論文，以及在我讀碩班的兩年期間的教導。也非常感謝我的口試委員徐立中老師和鄭旭辰老師的幫助，提出很多很好的建議使這篇論文得以更加完善。

由衷感謝實驗室的成員，包括剛進入分醫所時，手把手帶我做實驗的芝妤學姊、李緯，在實驗上以及實驗室中的大小事給予了非常多幫助的林芷學姊、哲炫、書偉、家芸、昱晴、珮琪。另外，也對實驗過程中果蠅們的犧牲感激在心。

最後，感謝家人們的全力支持，讓我沒有後顧之憂地在分醫所學習並完成碩士論文及學位。

摘要



在脊椎動物和無脊椎動物的發育時期都被發現有神經重塑的過程，神經會接收外源及內源的刺激後引起重塑過程，將神經網路完善化並使其成為在成熟動物中可正常運作的迴路。樹突修剪是神經重塑的其中一種，並會發生在果蠅變態過程中的感覺神經元。果蠅感覺神經元的樹突修剪需要 Ik2 激酶和其下游的調控因子 Spn-F。在此篇研究中，已知在胞吐和再循環過程中扮演重要角色的小 GTP 酶 Rab11 被發現作為樹突修剪和樹突型態發生重要的調控因子。此外，我們也藉由基因實驗和蛋白質成像實驗發現 Rab11 在樹突修剪中可能有需要倚靠 Spn-F 的功能及不須倚靠 Spn-F 的功能，其中 Rab11 不須倚靠 Spn-F 的功能是參與在負向調控細胞膜上的其中一種細胞黏附分子，Nrg。最後，我們也發現三個已知的 Rab11 鳥嘌呤核苷酸轉換因子有參與在調控樹突型態發生。總結來說，此篇研究指出了 Rab11 在神經網路的建立及重塑皆扮演著不可或缺的角色。

關鍵字：神經重塑，樹突修剪，樹突型態發生，Ik2 激酶，Spn-F，Rab11，

Crag，Parcas，TRAPP complex II，Nrg

Abstract



During development, neuronal remodeling refines neuronal networks in response to external and internal stimuli to establish fully functioning wiring in both vertebrates and invertebrates. Dendrite pruning, which is one of the remodeling processes, occurs in *Drosophila* sensory neurons during metamorphosis and this pruning process requires Ik2 kinase and its downstream regulator, Spindle-F (Spn-F). Here we demonstrate that a small GTPase Rab11, a regulator in exocytic and recycling pathway, is essential for both dendrite pruning and dendrite morphogenesis. Moreover, our genetic studies and protein imaging experiments revealed that Rab11 could have a Spn-F-dependent function and a Spn-F-independent function, which involves in the degradation of a cell-adhesion molecule Neuroglian (Nrg), in dendrite pruning. Also, we identified three Rab11 guanine nucleotide exchange factors (GEFs) as regulators for dendrite morphogenesis. Altogether, we point out the importance of Rab11 in both establishment and refinement of neuronal networks.

Keywords: neuronal remodeling, dendrite pruning, dendrite morphogenesis, Ik2 kinase, Spindle-F (Spn-F), Rab11, Crag, Parcas, transport protein particle (TRAPP) complex II, Neuroglian (Nrg)

Contents



誌謝.....	i
摘要.....	ii
Abstract.....	iii
Contents.....	iv
List of Figures.....	vi
List of Tables.....	vii
Introduction.....	1
Developmental neuronal remodeling.....	1
Neurite pruning.....	2
Dendrite pruning of sensory neurons in <i>Drosophila</i>	3
Ik2/Spn-F pathway in dendrite pruning of <i>Drosophila</i>	5
Rab11 and its roles in cellular trafficking.....	6
Methods.....	8
Results.....	14
Rab11 GTPase is required for dendrite pruning in ddaC neurons.....	14
Rab11 is crucial for dendrite morphogenesis in ddaC neurons.....	15
Rab11 is indeed required for dendrite pruning in ddaC neurons.....	16
Dendrite pruning defects were not found in the ddaC neurons with mutation of the	

known Rab11 GEFs genes.....	18
The three known Rab11 GEFs participate in regulation of dendrite morphogenesis in ddaC neurons.....	19
Endocytosis is impaired in <i>Rab11</i> mutant neurons.....	20
The Nrg-internalizing endocytic pathway is impaired in <i>Rab11</i> mutant neurons...	23
Spn-F is not required for maintaining Nrg-internalizing endocytic pathway in dendrite pruning of ddaC neurons.....	24
There is a genetic interaction between <i>Rab11</i> and <i>spn-F</i> in dendrite pruning of ddaC neurons.....	25
Ik2 kinase activation and Spn-F dispersion are normal in <i>Rab11</i> mutant neurons..	26
The Rab11-interacting domain of Spn-F is crucial for dendrite pruning in ddaC neurons.....	28
Discussion.....	30
Reference.....	40
Figures.....	51
Tables.....	84

List of Figures



Figure 1. Rab11 GTPase is required for dendrite pruning in ddaC neurons.....	51
Figure 2. Rab11 is crucial for dendrite morphogenesis in ddaC neurons.....	53
Figure 3. Rab11 is indeed required for dendrite pruning in ddaC neurons.....	56
Figure 4. The three known Rab11 GEFs participate in regulation of dendrite morphogenesis in ddaC neurons.....	61
Figure 5. Endocytosis is impaired in <i>Rab11</i> mutant neurons.....	66
Figure 6. The Nrg-internalizing endocytic pathway is impaired in <i>Rab11</i> mutant neurons.....	70
Figure 7. Spn-F is not required for maintaining Nrg-internalizing endocytic pathway in dendrite pruning of ddaC neurons.....	73
Figure 8. There is a genetic interaction between <i>Rab11</i> and <i>spn-F</i> in dendrite pruning of ddaC neurons.....	76
Figure 9. Ik2 kinase activation and Spn-F dispersion are normal in <i>Rab11</i> mutant neurons.....	78
Figure 10. The Rab11-interacting domain of Spn-F is crucial for dendrite pruning in ddaC neurons.....	80
Figure 11. Proposed model of the roles of Rab11 in dendrite pruning in ddaC neurons.....	83

List of Tables



Table 1. Dendrite pruning defects were not found in the ddaC neurons with mutation of	
the known Rab11 GEFs genes.....	84

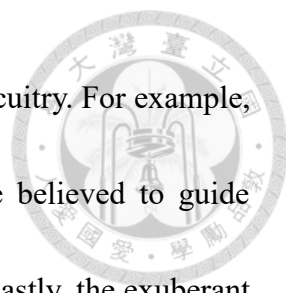
Introduction



Developmental neuronal remodeling

During the development of nervous systems, exuberant neuronal network is established by progressive events, including neurogenesis, neurites outgrowth and axon guidance. After establishing primary neuronal network, neuronal network is further remodeled through regressive events, such as synapses elimination, neurite pruning and programmed cell death, for the refinement and precise wiring of neuronal network in both invertebrates and vertebrates (Yu & Schuldiner, 2014) (Cowan et al., 1984).

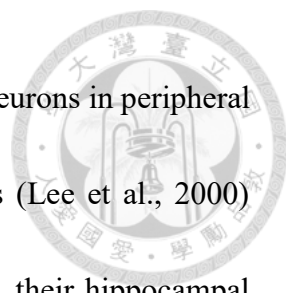
It is still not completely understood why so many animal species require remodeling processes to generate mature neuronal network. Nonetheless, it has been proposed that the reasons why remodeling processes are acquired by neuronal development are different in each neuronal system (Schuldiner & Yaron, 2015). Several examples are elaborated below to give insights into the potential reasons why neurons remodel themselves during development. Firstly, in *Drosophila melanogaster*, the remodeling of their mechanosensory neurons during metamorphosis is proposed to separate the neuronal networks required for sensing different inputs in larval and adult stages. The separation of sensory networks could underlie the different behaviors of larvae and adults. Therefore, remodeling process could serve as a switch for animal behaviors at different stages in this case (Consoulas et al., 2000). Secondly, pre-remodeled neuronal connections could serve



transient functions, such as guiding other neurons, in establishing circuitry. For example, the transient thalamic afferents originating from telencephalon are believed to guide thalamocortical axons growth in rodents (Innocenti & Price, 2005) Lastly, the exuberant pre-modeled connections could ensure proper connectivity after remodeling. During mammalian neuromuscular junctions (NMJ) development, each NMJ is innervated by approximately ten axons at birth and further reduced to one axon per NMJ through pruning postnatally. The exuberant connections at NMJ before remodeling is proposed to produce enough synaptic release sites, which are taken over by the remaining axon after remodeling, for motor signal transduction and thereby ensure proper connectivity in mature animals (Tapia et al., 2012).

Neurite pruning

One of the remodeling processes, neurite pruning, is a process in which neurites are eliminated without causing cell death, and it is observed in both invertebrates and vertebrates (Thompson & Nelson, 2001) In holometabolous insects like *Drosophila*, their body composition and structures undergo massive transformation and their neuronal network perform large-scale remodeling, including pruning, during metamorphosis. Specifically, their mushroom body (MB) γ neurons, embryonic olfactory projection neurons and serotonergic neurons in central nervous system undergo axon and dendrite

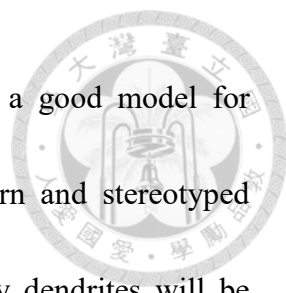


pruning, and their class I and IV dendritic arborization (da) sensory neurons in peripheral nervous system (PNS) prune larval dendrite during metamorphosis (Lee et al., 2000) (Marin et al., 2005) (Singh et al., 2010) (Kuo et al., 2005). In mice, their hippocampal infrapyramidal bundle and hippocampo-septal projections undergo axon pruning during postnatal development (Bagri et al., 2003). In humans, synaptic “blooming and pruning” take place in various cortical areas postnatal and continue until puberty (Thompson & Nelson, 2001).

It has been found that pruning defects would cause disruption of nervous functions in animals and neurological diseases or abnormalities in humans. For example, the pruning defects of climbing fibers in mouse cerebellum result in defects in motor learning (Kakegawa et al., 2015). In addition, improper pruning in humans has been linked to schizophrenia (Cocchi et al., 2016), autism (Tang et al., 2014), and synesthesia (Rouw et al., 2007). Given that dysfunctions manifest when pruning is dysregulated, pruning is deemed as an essential process during development to sculpt proper wiring in nervous system.

Dendrite pruning of sensory neurons in *Drosophila*

Our lab focuses on studying dendrite pruning in *Drosophila*. In *Drosophila* PNS, dendrite pruning occurs in three dorsal da neurons, including ddaD/E (class I) neurons



and ddaC (class IV) neurons. Among them, ddaC neurons make a good model for studying dendrite pruning, given their elaborated branching pattern and stereotyped schedule of pruning process. During metamorphosis, their primary dendrites will be severed at 5-10h after puparium formation (APF), and the detached dendrites will thereafter become fragmented and eventually be phagocytosed by nearby epidermal cells at 16-18h APF, leaving the soma and attaching axon intact. After pruning, ddaC neurons regrow their adult-specific dendrites to cover the body surface (Kuo et al., 2005) (Han et al., 2014) (Yu & Schuldiner, 2014).

Many studies have focused on ddaC neurons to study dendrite pruning. However, the molecular mechanism underlying the pruning process is still largely unknown. It has been known that ecdysone, the central regulator of metamorphosis, and its receptors are required for the initiation of dendrite pruning in ddaC neurons (Kuo et al., 2005). The ecdysone signaling will turn on the expression of certain pruning factors, such as Sox14, Mical, headcase, and Fos, to mediate dendrite pruning (Kirilly et al., 2009) (Loncle & Williams, 2012) (Zhu et al., 2009), and also increase Ik2 kinase activity by unknown mechanism (Lin et al., 2015). Various other mechanisms are also required for dendrite pruning at specific time and location in neurons, including ubiquitin-proteasome system (Kuo et al., 2005) (Kuo et al., 2006) (Wong et al., 2013), caspase activity (Kuo et al., 2006), compartmentalized calcium transients (Kanamori et al., 2013), local endocytosis

(Kanamori et al., 2015), global endocytosis of Nrg (Zhang et al., 2014), and microtubule (MT) severing protein Katanin p60-like 1 (Lee et al., 2009). However, how these mechanisms coordinate with each other to mediate dendrite pruning is still poorly understood.

Ik2/Spn-F pathway in dendrite pruning of *Drosophila*

In our previous study, we identified *Drosophila* IKK-related kinase (Ik2) as an essential component in dendrite pruning. In early pupae, Ik2 is somehow activated by ecdysone, the master regulator of metamorphosis. After being activated, Ik2 phosphorylates Spindle-F (Spn-F), an arthropod-conserved coil-coiled protein, and results in dispersion of Spn-F puncta, which exist in larval ddaC neurons (Lee et al., 2009) (Lin et al., 2015). The experiments conducted by lab alumni further showed that Spn-F puncta co-localize with Rab11, a regulator of recycling endosomes, in larval ddaC neurons.

Ik2 and Spn-F has also been found to participate in other development processes in *Drosophila*, such as oogenesis and bristle elongation. During oogenesis, Ik2 interacts and phosphorylates Spn-F to regulate cytoskeleton organization (Dubin-Bar et al., 2008). Moreover, Ik2 and Spn-F regulate mRNA localization through affecting actin and MT minus-end organization during oogenesis (Shapiro & Anderson et al., 2006) (Abdu et

al.,2006). During bristle elongation, both Ik2 and Spn-F were proposed to promote axial growth of bristle through regulating MT functions (Abdu et al.,2006) (Bitan et al., 2010).



Rab11 and its roles in cellular trafficking

Rab11 has been shown to participate in exocytic and recycling processes to direct proteins or membranes toward plasma membrane. Rab11 proteins mediate exocytic process at trans-Golgi network (TGN) and post-Golgi vesicles, and regulate recycling process at pericentriolar recycling endosomes (Urbé et al., 1993). The trafficking of Rab11-positive vesicles is achieved through Rab11 forming complexes with motor proteins and thereby being transported on cytoskeletons such as MTs and actins/myosin (Welz et al., 2014).

Rab11 belongs to the small GTPase family, and this family of proteins undergo state-switching between GTP-bound active state and GDP-bound inactive state. To switch between these two states, specific enzymes are required. Guanine nucleotide exchange factors (GEFs) exchange the Rab protein-bound GDP with GTP to turn Rab proteins into active state. GTPase-activating proteins (GAPs) catalyze the internal GTPase activity of Rab proteins, so the Rab proteins-bound GTP is hydrolyzed and the Rab proteins thereby become inactive GDP-bound state. There is conformational change when Rab proteins undergo state-switching. In most cases, the conformation of Rab proteins in GTP-bound

active state allows them to interact with effector proteins and perform their functions (Zhen & Stenmark, 2015).



Here, we identified Rab11, a Spn-F-associated protein, as a crucial component for dendrite pruning and dendrite morphogenesis of ddaC neurons. Our data suggest that Rab11 could mediate pruning in both Spn-F-dependent and Spn-F-independent manners. The Spn-F-independent function of Rab11 is to maintain Nrg-internalizing endocytic pathway during pruning. We also show that three Rab11 GEFs are regulators for dendrite morphogenesis. Overall, our results raise the possibility that both progressive establishment and regressive remodeling of neuronal network require Rab11-associated exocytic/recycling trafficking activity.

Methods



Fly strains

Most crosses were conducted at 25°C. Several crosses mentioned in Fig 5F, G were performed at 18°C. For the visualization of class IV da neurons, *ppk-GAL4* (Grueber et al., 2007), *UAS-mCD8GFP*, *ppk-CD4-tdTom* (Bloomington Drosophila Stock Center (BDSC) #35845), *ppk-eGFP* (Grueber et al., 2003) were used. The other fly strains used in this study include: *w¹¹¹⁸*; *UAS-Luciferase-dsRNA* (BDSC #31603); *UAS-Rab11-dsRNA* (Vienna Drosophila Resource Center #108382); *UAS-lacZ*; *GSG2295* (BDSC #40266); *Crag^A*, *FRT19A* (BDSC #52346); *sn*, *FRT19A* (BDSC #1740); *tubP-Gal80*, *FRT19A* (BDSC #42726); *hsFLP1*, *tubP-Gal80*, *FRT19A* (BDSC #5132, 5133); *SOP-FLP* (Kyoto Stock Center #109944), *pcs^{gs}* (a gift from Dr. M.K. Baylies); *ficp*, *pcs^{gs}* (a gift from Dr. D. Yamamoto); *Df(2L)Exel7078* (BDSC #7851); *brun^{Z0704}* (BDSC #66721); *brun^{Z3358}* (BDSC #66720); *UAS-2xFYVE-GFP* (BDSC #42712); *UAS-Rab5-GFP* (BDSC #43336); *UAS-Rab5-DN* (BDSC #42703); *spn-F-dsRNA* (National Institute of Genetics #12114R-4); *spn-F²* (Abdu et al., 2006); *Rab11^{ΔFRT}* (a gift from Dr. O. Schuldiner)(Bogard et al., 2007); *UAS-DmIKKεIR* (Kuranaga et al., 2006). Transgenic flies *UAS-Rab11-GFP*; *UAS-Rab11-CA-GFP*; *UAS-Rab11-DN-GFP*; *UAS-spn-F-mCherry*; *UAS-spn-F-ΔSCD* were generated through P-element-mediated transformation by former lab members.

Live imaging of larvae and pupae



Third instar larvae were washed with ddH₂O and placed on microscope slides. 170 μ l 90% glycerol was poured onto the larvae and then long coverslips (24 x 55 mm) were used to squeeze them until the coverslips tightly attached to the slides. The imaging of larvae must be completed within twenty minutes after squeezing in case that the neuronal death commenced. 16h APF pupae were placed on a strip of tape, and then pupal case was removed using forceps. The pupae inside were transferred onto a microscope slide and immersed with a drop of ddH₂O. High vacuum grease (DOW CORNING) was applied around pupae, and then the pupae were covered with coverslips for subsequent imaging. Imaging of larval and pupal neurons was done by confocal microscope (Zeiss LSM 700). Images were obtained by Z-stacking and maximum intensity projection through Zen software (Zeiss). The brightness and contrast were adjusted by Photoshop (Adobe).

Evaluation of pruning phenotypes

Since the clearance of the severed dendrites completes around 16–18 APF (Yu & Schuldiner, 2014), we examined the pruning phenotypes of ddaC neurons at 16h APF. Pruning defects are defined as the persistence of any soma-attached dendrites (length > 100 μ m) at 16h APF.

Analysis of larval dendritic morphology

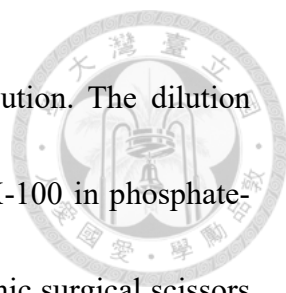
All the images of larval neurons were pre-processed before analyzing dendritic morphology. The pre-processing was conducted through tracing all the dendritic branches by “Simple Neurite Tracer” plugin in ImageJ (Schindelin et al., 2012). The traced paths were then skeletonized for further analysis. Sholl analysis and Strahler analysis were done by Fiji plugins of ImageJ. Area of dendritic coverage was measured by ImageJ and the average dendritic covering area of control neurons in each experiment was assigned as 100. The number of neurons examined was four for each group.

GeneSwitch experiments

The parent flies were transferred consecutively from one vial to another at 4-hour intervals to unify the developing stages of the progeny larvae in every single vial. The larvae were transferred to food containing 240 $\mu\text{g/ml}$ RU486 (Sigma) at about 84h AEL or 96h AEL with forceps. The larvae would continuously consume the RU486-containing food until being imaged or pupation. RU486 was a gift from Dr. C.T. Chien.

Immunohistochemistry

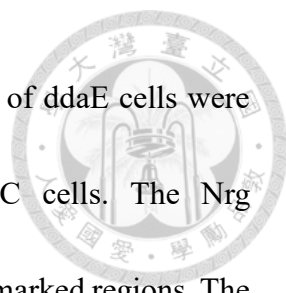
Primary antibody used in this study was mouse anti-Nrg antibodies (BP104, DSHB) with 1:20 dilution. Secondary antibody used in this study was Cy3-conjugated donkey



anti-mouse IgG (H+L) (Jackson ImmunoResearch) with 1:500 dilution. The dilution buffer for antibodies was washing solution, which is 0.3% Triton X-100 in phosphate-buffered saline (PBS). Larvae and pupae were dissected by ophthalmic surgical scissors in 4°C 1X PBS. During dissection, larvae and pupae were placed with their ventral side up and fixed with metal pins, and then they were cut open through midline, thereby creating two leaflets of abdominal epidermis and muscle. After being cleaned out all the internal organs and fat bodies inside, the remaining leaflets immediately underwent fixation with cold 4% formaldehyde for 20 minutes. Following fixation, samples were immersed in blocking solution, which is 5% normal donkey serum (Jackson ImmunoResearch), for 1 hour at 4°C. Subsequently, samples were stained with primary antibodies overnight at 4°C and then treated with secondary antibodies for 2 hours at room temperature. Samples were thoroughly washed with washing solution after fixation and staining.

Quantification of immunohistochemistry

For the quantification of Nrg level on somatic cell surface, the images were first split into different fluorescent channels by ImageJ. The images in red channel, which labeled Nrg, underwent background subtraction (rolling ball radius = 50) before analyzing. The somatic cell surface regions of ddaC cells were marked by line tool according to the green



channel, which labeled ddaC cells. The somatic cell surface regions of ddaE cells were marked according to their relatively posterior location to ddaC cells. The Nrg immunostaining intensities were measured as mean gray value at the marked regions. The measured Nrg immunostaining intensities of ddaC cells were normalized to those of ddaE cells on the same images, since ddaE cells are also destined for dendrite pruning without expression of mutant transgenes (Fig 6). The Nrg immunostaining intensities were measured in the wild-type and *spn-F²* ddaC cells, which were scanned with similar laser intensities and gains, without normalization (Fig 7D-F).

Time-lapse imaging and Spn-F dispersion quantification

In the experiments of time-lapse imaging of Spn-F-mCherry dispersion in same ddaC neurons from larvae to early pupae, third instar larvae were mounted on 5% agarose pad with dorsal side up. Subsequently, they were immersed with 90% glycerol and covered by coverslips. The larval ddaC neurons were imaged once and then the same pupal neurons were imaged at 30-minute intervals until 4h APF. For quantification of the cytosolic fluorescence intensities of Spn-F-mCherry in soma, we drew 3-5 lines in cytosol on each image by the profile analysis module of the Zen software (Zeiss). According to the drawn lines, we calculated the average signal intensities (a.u./ μm) on them. Spn-F-mCherry puncta represented as peaks of fluorescence intensities, which were excluded

from calculation, and the rest of the signal was considered as the dispersed cytosolic Spn-F-mCherry. The average Spn-F-mCherry cytosolic fluorescence intensities in larval neurons of each group was assigned as one to calculate the fold changes in the same neuron at different timepoints.

Statistical analysis and graph plotting

Statistical analyses were performed and graphs were generated in GraphPad Prism. Error bars in all graphs represent SD. P values were shown in graphs as follows: ****, $p < 0.0001$; ***, $p < 0.001$; **, $p < 0.01$; *, $p < 0.05$; n.s., not significant. Two-way ANOVA with Dunnett's multiple comparisons test (Fig 2E), with Tukey's multiple comparisons test (Fig 4L-N) or with Sidak's multiple comparison test (Fig 7F) was performed. Ordinary one-way ANOVA with Dunnett's multiple comparisons test (Fig 2F, 3F, 4P, 6I, 6J) or with Tukey's multiple comparisons test (Fig 4Q, 5G, 8A) was performed. Unpaired two-tailed t test with (Fig 5J, 7C) or without (Fig 4O) Welch's correction was performed.

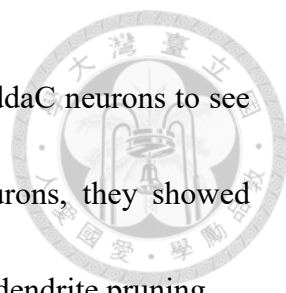
Results

Rab11 GTPase is required for dendrite pruning in ddaC neurons



Our previous observation that Spn-F exhibits punctate pattern in larval ddaC neurons (Lin et al., 2015) made us speculate whether Spn-F puncta localize with cellular organelles, so we expressed several organellar markers with Spn-F-mCherry to examine the co-localization. When co-expressing Spn-F-mCherry with Rab11-YFP, which marked recycling endosomes, in ddaC neurons, we found co-localization between them (data not shown).

In order to figure out whether Rab11 also plays a role in dendrite pruning, we investigated the pruning phenotypes in neurons with Rab11 perturbation. We used *ppk-GAL4*, a Class IV da neurons-specific GAL4 driver line (Ainsley et al., 2003) for expressing *Rab11-dsRNA* in ddaC neurons to perform RNA interference (RNAi). In the neurons with *Rab11* RNAi, the dendrites were still attached to soma at 16h APF, when all the dendrites were removed in the control neurons (Fig 1A, B, D), suggesting that Rab11 is required for dendrite pruning in ddaC neurons. To further confirm this, we searched for other means for perturbing Rab11 function. Small GTPases like Rab11 are known to switch between active GTP-bound form and inactive GDP-bound form (Goody et al., 2017), and being locked in GDP-bound form is known to perturb their functions (Zhang et al., 2007). Therefore, we expressed dominant negative (DN) Rab11 mutant protein



(S25N), which is defective in GTP binding (Zhang et al., 2007), in ddaC neurons to see if pruning was affected. When over-expressing Rab11-DN in neurons, they showed severing defects (Fig 1C, D), supporting that Rab11 is important for dendrite pruning.

Rab11 is crucial for dendrite morphogenesis in ddaC neurons

Besides observing pruning phenotypes in pupal stage, we also checked dendritic morphology of *Rab11* mutant ddaC neurons in third instar larvae. We applied Sholl analysis and Strahler analysis to measure dendritic branching complexity. Sholl analysis was performed by overlaying concentric rings on the images taken from neurons and calculating the number of times that concentric rings intersect with dendritic branches. Strahler analysis was conducted by counting the number of branches with different orders. Moreover, the area of dendritic coverage was also measured to quantify the extent of dendrite outgrowth. In the control neurons, dendrites showed highly complex branching and extensive coverage of the dorsal epidermal surface (Fig 2A, D, E). However, in neurons with *Rab11* RNAi and Rab11-DN expression, the larval dendritic morphology manifested reduced distal dendritic branches and area of coverage (Fig 2B-F). Also, when applying Sholl analysis, we found the radius with maximal intersections shorter in neurons with *Rab11* RNAi and Rab11-DN expression (Fig 2D), indicating a major loss

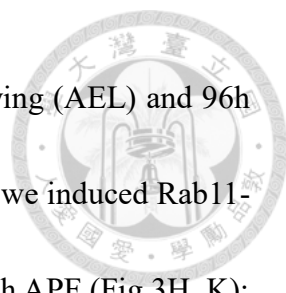
of distal dendrites. These data suggested that Rab11 is also important for dendrite morphogenesis and outgrowth in larval neurons.



Rab11 is indeed required for dendrite pruning in ddaC neurons

Since there was a reduction of dendritic branching and covering area in larval neurons with Rab11 perturbation, we could not exclude the possibility that the pruning defects we observed in pupal stage arose from those larval morphological defects. To bypass the effects of Rab11 perturbation on dendrite morphogenesis and examine the direct effects of Rab11 perturbation on dendrite pruning, we used GeneSwitch technique, which is modified from GAL4-UAS system and can induce temporal expression of desired transgenes by chemical administration. GeneSwitch GAL4 is composed of GAL4 DNA-binding domain, human progesterone receptor (hPR) ligand-binding domain and NF- κ B transcription activation domain. Upon feeding the flies or larvae with RU486, a hPR antagonist, RU486 will bind to the hPR ligand-binding domain of GeneSwitch GAL4 and induce a conformational change of GeneSwitch GAL4. Then it becomes transcriptionally active and can thereby induce UAS transgenes expression (Nicholson et al., 2008).

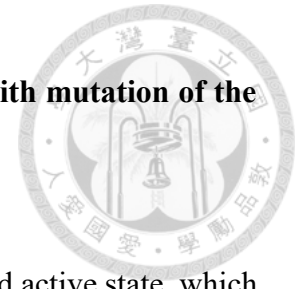
We decided to induce Rab11-DN expression with RU486 in third instar larvae whose dendrite morphogenesis would almost complete at that stage. Not knowing how long should the induction period span to sufficiently disrupt pruning without disturbing



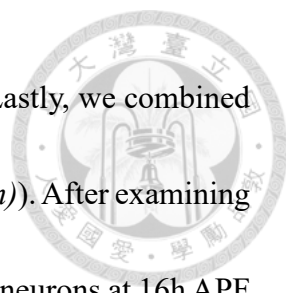
dendrite morphogenesis, we chose two timepoints, 84h after egg-laying (AEL) and 96h AEL, to start feeding the larvae with RU486-containing food. When we induced Rab11-DN expression at 84h AEL, pruning was successfully disturbed at 16h APF (Fig 3H, K); however, the larval dendrites exhibited reduced distal dendritic branches and area of coverage when being inspected just before pupation (Fig 3B, E, F). On the other hand, when we induced Rab11-DN at 96h AEL, the neurons also showed pruning defects (Fig 3I, K), and yet their dendritic branching and covering area remained unaffected when compared to those in larvae without induction (Fig 3A, C, E, F). With regards to this, we successfully bypassed the effect of Rab11-DN on larval dendrite morphogenesis and still observed pruning defects in pupae in the group of induction at 96h AEL, which indicates that Rab11 is indeed required for dendrite pruning in pupae.

In order to confirm whether pruning was affected by RU486 administration alone, we used GeneSwitch to express Rab11-wt, whose expression does not cause pruning defects (data not shown), at 96h AEL. After inducing Rab11-wt expression with RU486 at 96h AEL, the neurons showed normal larval dendritic morphology (Fig 3D-F) and pruning (Fig. 3H, I) as Rab11-DN non-induction neurons did (Fig 3A, E, F, G, K), suggesting RU486 administration has no effects on dendrite pruning.

Dendrite pruning defects were not found in the ddaC neurons with mutation of the known Rab11 GEFs genes



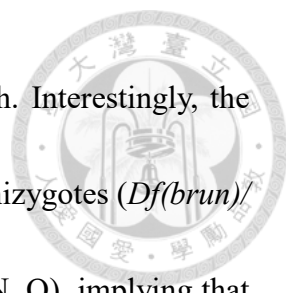
Most small GTPases perform their functions through GTP-bound active state, which can be promoted by either activating GEFs or inhibiting GAPs. Since most Rab GTPases possess high intrinsic rates at hydrolyzing GTP, GAPs are generally considered less critical than GEFs (Barr & Lambright, 2010). With regards to this, we investigated the potential roles of Rab11 GEFs in dendrite pruning. To date, three Rab11 GEFs have been identified in *Drosophila melanogaster*. These Rab11 GEFs are Crag, Parcas (encoded by *pcs*) and transport protein particle (TRAPP) complex II (Xiong et al., 2012) (Riedel et al., 2017). To verify if these Rab11 GEFs play roles in dendrite pruning, we examined the pruning phenotypes in ddaC cells with mutation of these Rab11 GEFs genes. For *Crag* mutant allele, we used *Crag^A*, a loss-of-function allele, and generated homozygous *Crag^A* mutant clones by inducing mitotic recombination with Mosaic analysis with a repressible cell marker (MARCM) technique (Lee & Luo, 1999), since *Crag^A* mutant flies are homozygous viable only until second instar larval stage (Xiong et al., 2012). For *pcs* mutant allele, we applied mutants homozygous for a *pcs* null allele, *pcs^{gs}*. For TRAPP complex II mutant, we chose alleles containing mutation for *brunelleschi* (*brun*), which encodes a TRAPP complex II-specific subunit, TRAPPC9. We generated *brun* hemizygotes, which contained a *brun* loss-of-function allele (*brun^{Z0704}* or *brun^{Z3358}*, both



encode truncated TRAPPC9) and a *brun*-deleted allele (*Df (brun)*). Lastly, we combined *pcs^{gs}* and *Df (brun)* to create transheterozygous mutant (*pcs^{gs}/Df (brun)*). After examining the *crag*, *pcs* and *brun* mutants, we found no pruning defects in ddaC neurons at 16h APF (Table 1). This indicates that these Rab11 GEFs may not be required for dendrite pruning and implies that there may be other unknown Rab11 GEFs governing pruning process. Nevertheless, it is also possible that these three Rab11 GEFs function redundantly with each other and/or with other unknown Rab11 GEFs in dendrite pruning of ddaC neurons.

The three known Rab11 GEFs participate in regulation of dendrite morphogenesis in ddaC neurons

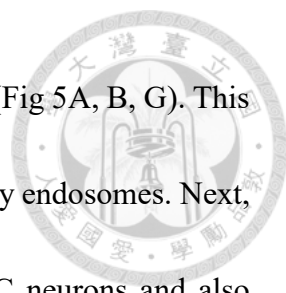
Since Rab11 participates in larval dendrite morphogenesis in ddaC neurons (Fig 2), Rab11 GEFs could cooperatively mediate the same function. To explore this possibility, we inspected the larval dendritic morphology in neurons with Rab11 GEFs mutation mentioned above. In *Crag^A* MARCM clones, there were significantly more distal dendrites and area of coverage compared to the control MARCM clones (Fig 4A, B, I, L, O), indicating Crag could be a negative regulator in dendrite branching and outgrowth. On the contrary, there were significantly reduced distal dendrites and area of coverage in *pcs^{gs}* homozygotes and *brun* hemizygous mutants (*brun^{Z0704}/Df (brun)*, *brun^{Z3358}/Df (brun)*)(Fig 4C-G, J, K, M, N, P, Q), suggesting Parcas and TRAPP complex II are both




required in positive regulation of dendrite branching and outgrowth. Interestingly, the dendritic branching and outgrowth were already reduced in *brun* hemizygotes (*Df(brun)/+*) when compared to *pcs^{gs}* heterozygotes (*pcs^{gs}/+*) (Fig 4C, E, K, N, Q), implying that *brun* is haploinsufficient in mediating dendrite morphogenesis. These results reveal that Crag could be a negative regulator for dendrite morphogenesis, whereas Parcas and TRAPP complex II could be positive regulators for dendrite morphogenesis.

Endocytosis is impaired in *Rab11* mutant neurons

It has been found that endocytic pathway is essential for dendrite pruning in ddaC neurons (Zhang et al., 2014) (Kanamori et al., 2015). Since Rab11 is an important component of recycling pathway in endocytic networks, we asked whether Rab11 perturbation affects endocytic pathway in dendrite pruning. To answer this question, we applied an early endosome marker 2xFYVE-GFP. The FYVE domain can specifically bind to phosphatidylinositol 3-phosphate, which is a phospholipid generated and enriched on the membrane of early endosomes and internal vesicles of multi-vesicular bodies (Gillooly et al., 2000). To verify this marker, we co-expressed 2xFYVE-GFP and Rab5-DN (S43N), whose expression would block the formation of early endosomes (Stenmark et al., 1994) (Zhang et al., 2007), in ddaC neurons. The number of 2xFYVE-GFP puncta in soma significantly decreased and the GFP signal became diffuse in cytosol in Rab5-



DN-expressing neurons when compared to lacZ-expressing neurons (Fig 5A, B, G). This finding supported that 2xFYVE-GFP could serve as a marker for early endosomes. Next, we co-expressed 2xFYVE-GFP protein and *Rab11-dsRNAs* in ddaC neurons and also found reduced 2xFYVE-GFP puncta number in some of the neurons when compared to the neurons co-expressed with *Luciferase-dsRNAs* (Fig 5C, E). This data suggests that endocytosis might somehow be interrupted when Rab11 is perturbed. However, the patterns of 2xFYVE-GFP puncta was heterogeneous among individual *Rab11* RNAi neurons. We categorized these patterns into three types: type 1 for the neurons with more than twenty 2xFYVE-GFP puncta (Fig 5D, F); type 2 for those with less than fifteen 2xFYVE-GFP puncta (Fig 5E, F); type 3 for those with no observable 2xFYVE-GFP puncta (image not shown, Fig 5F). We speculated that the heterogeneous patterns of 2xFYVE-GFP puncta in *Rab11* RNAi neurons could result from different extent of RNA interference among individual neurons. Specifically, the type 2 and type 3 patterns could be caused by stronger effect of RNA interference. To verify this, we tried to restrict the effect of *Rab11* RNA interference by raising the larvae at 18°C instead of 25°C (Fortier & Belote, 2000) and examined whether the endosomal defects would be mitigated. After doing so, none of the *Rab11* RNAi neurons manifested type 3 pattern and the percentage of neurons with type 1 pattern increased (Fig 5F), which showed mitigated endosomal defects. This supported that the differential 2xFYVE-GFP patterns were due to different

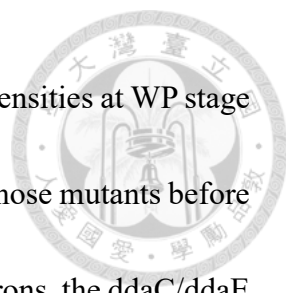


extent of *Rab11* RNA interference. Subsequently, we counted the 2xFYVE-GFP puncta number in these *Rab11* RNAi neurons and found a mild but significant decrease of 2xFYVE-GFP puncta number when compared with that in *Luciferase* RNAi neurons (Fig 5G). This further supported that endocytosis is defective when Rab11 is perturbed. Nevertheless, the *Rab11* RNAi neurons did not show diffuse cytosolic 2xFYVE-GFP signal as Rab5-DN-expressing neurons did (Fig 5B, D, E). This implies that the expression level of 2xFYVE-GFP could be low in the first place when knocking down Rab11, which raises the possibility that the endosomal defects we observed were faked by low expression of the marker.

To investigate whether Rab11 perturbation could actually reduce the number of early endosomes, we applied another early endosome marker, Rab5-GFP. In *Rab11* RNAi neurons, the expression pattern of Rab5-GFP was homogeneous and the number of Rab5-GFP puncta was significantly reduced when compared with that of *Luciferase* RNAi neurons (Fig 5H, I, J). These data suggest that endocytosis is disturbed when Rab11 is perturbed and imply that the endocytic pathway of dendrite pruning could also be disrupted after Rab11 perturbation.

The Nrg-internalizing endocytic pathway is impaired in *Rab11* mutant neurons

The Rab5-dependent endocytic pathway in dendrite pruning is to mediate internalization of Nrg in early pupae (Zhang et al., 2014). Since the number of early endosomes is already reduced in *Rab11* RNAi larval neurons (Fig 5), we next asked whether the endocytosis of Nrg in early pupae is also affected after Rab11 perturbation. To visualize Nrg molecules and their locations in neurons, we performed Nrg antibody staining. In wild-type neurons, we found that most Nrg on the cell membrane are internalized into the cytoplasm at 5.5h APF (Fig 6A, B). Conversely, we observed that the internalization of Nrg was blocked at 5.5h APF in neurons expressing Rab5-DN (Fig 6C, D), which is consistent with the previous study (Zhang et al., 2014). Likewise, the Nrg internalization was also impeded at 5.5h APF when we expressed *Rab11-dsRNAs* or Rab11-DN in neurons (Fig 6E-H), indicating that Rab11 is required for proper downregulation of Nrg on plasma membrane. To further verify this finding, we analyzed the extent of Nrg retainment by quantifying the normalized ddaC/ddaE Nrg signal intensities in soma. We chose the Nrg signal of ddaE neurons for normalization because ddaE neurons had similar pruning fate without expressing the transgenes. The normalized signal intensities of Nrg were significantly higher in neurons with Rab5-DN, *Rab11-dsRNAs* or Rab11-DN expression than those in wild-type neurons at 5.5h APF (Fig 6I). It supports that Rab11 is required for Rab5-dependent Nrg-internalizing endocytic pathway



in dendrite pruning. Next, we measured the normalized Nrg signal intensities at WP stage to see if the amount of Nrg on the plasma membrane was affected in those mutants before Nrg internalization. In Rab5-DN- and Rab11-DN-expressing WP neurons, the ddaC/ddaE Nrg signal intensities were comparable to those in wild-type WP neurons. However, the ddaC/ddaE Nrg intensity values significantly increased in WP neurons with *Rab11* RNAi (Fig 6J), implying that Rab11 could be required for the equilibrium of plasma membrane-bound Nrg prior to dendrite pruning.


Spn-F is not required for maintaining Nrg-internalizing endocytic pathway in dendrite pruning of ddaC neurons

Since there is co-localization between Rab11 and Spn-F, which are both pruning mediators, in ddaC neurons, they could have a functional relationship in dendrite pruning. Considering this, we investigated if the Nrg-internalizing endocytic pathway, which Rab11 participates in, is dependent on Spn-F. First, we calculated the number of early endosomes detected by early endosome marker, 2xFYVE-GFP, in larval neurons with *spn-F* RNAi and found it comparable to that in neurons with *Luciferase* RNAi (Fig 7A-C), implying that the endocytic activity might not be affected after Spn-F perturbation. Next, we performed Nrg staining in *spn-F²* mutant neurons to examine Nrg internalization directly. In *spn-F²* mutant neurons, most of the Nrg on somatic plasma membrane during

WP stage was internalized at 5.5h APF (Fig 7D-F), which resembles wild-type neurons (Fig 6A, B; Fig 7F). These data collectively suggest that the Rab11-dependent Nrg-internalizing endocytic pathway in dendrite pruning is independent of Spn-F.

There is a genetic interaction between *Rab11* and *spn-F* in dendrite pruning of *ddaC* neurons

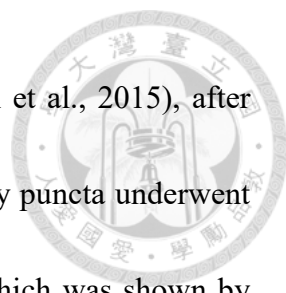
To gain more insight into the potential functional relationship between Rab11 and Spn-F, we next inquired whether there is a genetic interaction between them in dendrite pruning by comparing pruning phenotypes between *Rab11* or *spn-F* single mutants and their double mutants. When inspecting pruning phenotypes in *Rab11* and *spn-F* transheterozygous mutants, which contained a *Rab11* null allele and a *spn-F* loss-of-function allele (*Rab11*^{ΔFRT}/*spn-F*²), we found there was a significantly greater number of neurons with unsevered dendrites at 16h APF, compared to heterozygous mutants for either *Rab11* (*Rab11*^{ΔFRT}/+) and *spn-F* (*spn-F*²/+) (Fig 8A). Similarly, when introducing Rab11-DN or *Rab11-dsRNAs* expression into *spn-F*² background, there were enhanced pruning defects, which were shown by a higher percentage of neurons with unsevered dendrites than that of either *Rab11* or *spn-F* single mutants (Fig 8B). These aggravated pruning defects implied that there is a synergistic genetic interaction between *Rab11* and *spn-F*.



Since dendrite morphogenesis is impaired in Rab11-DN-expressing larval neurons (Fig 2C), the enhanced pruning defects in Rab11-DN-expressing *spn-F*² neurons may be caused by abnormal dendrite morphogenesis. To verify this, we applied GeneSwitch technique to bypass the effect of Rab11-DN expression on dendrite morphogenesis. We induced Rab11-DN expression temporally after 96h AEL, which is the Rab11-DN induction timepoint without disrupting dendritic morphology (Fig 3C), in *spn-F*² background. Likewise, Rab11-DN induction in *spn-F*² background still exacerbated pruning defects at 16h APF as compared to *spn-F*² alone or Rab11-DN induction in wild-type background (Fig 8C), supporting that there is indeed a synergistic genetic interaction between *Rab11* and *spn-F* in dendrite pruning. Although a synergistic interaction favors that the two proteins encoded by the interacting genes act in compensatory or parallel pathway (Mani et al., 2008), it is still likely that Rab11 also has a Spn-F-dependent function in dendrite pruning, given the co-localization and possible physical interaction between them.

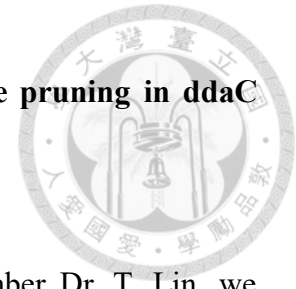
Ik2 kinase activation and Spn-F dispersion are normal in *Rab11* mutant neurons

To investigate the potential Spn-F-dependent function of Rab11 in dendrite pruning, we asked whether Rab11 participate in the Ik2/Spn-F pathway of dendrite pruning. To answer this question, we examined Spn-F puncta dispersion, which is dependent on



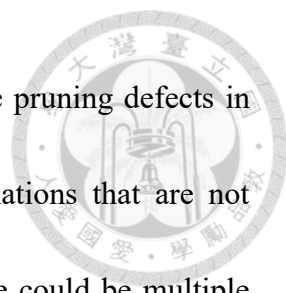
phosphorylation by Ik2 kinase in early pupae prior to pruning (Lin et al., 2015), after knocking down Rab11. In *Rab11* RNAi neurons, the Spn-F-mCherry puncta underwent dispersion during early pupation just like wild-type neurons did, which was shown by higher diffuse cytosolic fluorescence intensity and fewer puncta at 4h APF than at larval stage (Fig 9A-D), suggesting Rab11 does not participate in Ik2 activation and Spn-F dispersion. To corroborate this, we conducted time-lapse experiment by tracking single neurons from third instar larvae to 4h APF to monitor the change of cytosolic mCherry intensity during this time course. Consistent with the previous finding, we detected surges of mCherry cytosolic intensities, which indicate Spn-F dispersion, right after pupation in both wild-type neurons and *Rab11-dsRNAs*-expressing neurons (Fig 9E). Also, to confirm that the dispersion of Spn-F-mCherry is under the control of Ik2 kinase, we performed the same time-lapse experiment in *ik2* RNAi neurons, whose Spn-F dispersion would be inhibited (Lin et al., 2015). As expected, we failed to observe Spn-F-mCherry dispersion in neurons with *ik2* RNAi (Fig 9E), and thereby confirmed the dependency of Spn-F-mCherry dispersion on Ik2 kinase. Based on these findings, we can conclude that Ik2 activation and Spn-F dispersion are normal in *Rab11* mutant neurons, which suggests Rab11 does not act upstream of Ik2 activation and Spn-F dispersion in dendrite pruning. Nevertheless, there is still a possibility that Rab11 has a role downstream of Ik2/Spn-F complexes in dendrite pruning.

The Rab11-interacting domain of Spn-F is crucial for dendrite pruning in *ddaC* neurons



In the work from the doctoral thesis of our former lab member Dr. T. Lin, we confirmed that there is interaction between Spn-F and Rab11 and found that the Rab11-interacting domain in Spn-F is SpnF-conserved domain (SCD) (Fig 10A). To further examine whether Rab11 has Spn-F-dependent functions in dendrite pruning, we investigated the importance of the Rab11-interacting SCD domain in Spn-F in pruning. We utilized a truncated Spn-F mutant construct that delete the SCD domain (Spn-F- Δ SCD) (Fig 10A) to carry out the following experiments. After over-expressing Spn-F- Δ SCD, the *ddaC* neurons exhibited pruning defects, whereas the control neurons and Spn-F-wt-expressing neurons did not (Fig 10B). Moreover, the over-expression of Spn-F- Δ SCD failed to rescue the severing defects in *spn-F²* mutant neurons, while over-expression of Spn-F-wt could (Fig 10C). Collectively, these data pointed out that the Rab11-interacting domain in Spn-F has a crucial role in dendrite pruning and suggest that Rab11 could have a Spn-F-dependent function.

Since most small GTPases perform their functions through their active forms, the Spn-F-dependent function of Rab11 in dendrite pruning could also be performed through Rab11 activation. Inspired by this, we asked if over-expressing constitutively active (CA) form of Rab11 proteins could rescue the pruning defects in *spn-F²* mutant neurons. To



our surprise, the over-expression of Rab11-CA could not rescue the pruning defects in *spn-F*² mutant neurons (Fig 10D). There are two possible explanations that are not mutually exclusive for this result. The first explanation is that there could be multiple downstream targets for Spn-F in dendrite pruning, so rescuing Rab11 activation alone is not sufficient to compensate *spn-F* loss-of-function. The other explanation is that the Spn-F puncta dispersion in early pupae could simultaneously redistribute Rab11, so the loss-of-function Spn-F proteins may interfere with proper localization of active Rab11 molecules.

Discussion



Proposed roles of Rab11 in dendrite pruning in ddaC neurons

In this study, we found a small GTPase Rab11 important for dendrite pruning in ddaC cells. Our results suggest that Rab11 mediate pruning through at least two pathways, Spn-F-dependent and Spn-F-independent pathways. Through investigation on the localization of one membrane protein, Nrg, we propose that the Spn-F-independent function of Rab11 is required for Nrg-internalizing endocytic pathway (Fig 11). Still, there are unresolved questions deriving from the model we proposed. Firstly, the failure of rescuing pruning defects in *spn-F²* mutant neurons by Rab11-CA overexpression (Fig 10D) indicates there might be other downstream regulators in Ik2/Spn-F pathway other than Rab11. It will be of paramount importance to identify unknown regulators downstream of Ik2, given that Ik2 is the only known molecule causing precocious pruning in larvae (Lee et al., 2009). Secondly, the Spn-F-dependent function of Rab11 is unclear in this study. Since Spn-F undergoes dispersion in early pupae, it may mediate transportation of Rab11 or Rab11-positive vesicles. Lastly, how Rab11 is temporally regulated to mediate its Spn-F-independent function in Nrg internalization is also an intriguing question.




Disturbed dendrite morphogenesis may contribute to defective dendrite pruning

In the Rab11-DN GeneSwitch experiments, the pruning defects were more severe in the group of Rab11-DN induction at 84h AEL, whose dendritic morphology was abnormal (Fig 3B), when compared with the group of Rab11-DN induction at 96h AEL (Fig 3I). This higher incidence of unsevered dendrite might simply result from the greater level of Rab11-DN expression by longer induction period. The other possibility is that defective dendrite morphogenesis might partially contribute to pruning defects.

The potential roles of Rab11 GEFs or GTPase-activating proteins (GAPs) in dendrite pruning

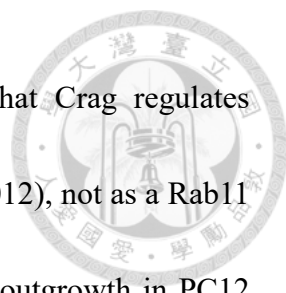
Our preliminary data (experiments conducted by former lab member Dr. T. Lin) showed that Rab11 activation is promoted by Ik2/Spn-F complexes, implying Rab11 activity could be temporally regulated through Ik2/Spn-F pathway during pruning. This potential temporal regulation could be achieved by either activation of GEFs or inhibition of GAPs. Based on the notion that GEFs are generally more crucial than GAPs (Barr & Lambright, 2010), and our previous finding (by Dr. T. Lin) that Spn-F has a stronger interaction with Rab11-GDP than Rab11-GTP, we think that Ik2/Spn-F more likely promote Rab11 activation through Rab11 GEFs. Although we did not observe pruning defects in the mutants for known Rab11 GEFs (Table 1), we could not rule out that Rab11



GEFs participate in pruning since there could be redundancy of Rab11 GEFs or unknown Rab11 GEFs promoting dendrite pruning. Considering the potential presence of unknown Rab11 GEFs, Spn-F may act as a Rab11 GEF itself and be activated after being phosphorylated by Ik2. To further address this question, in vitro GEF assay could be performed to see whether phosphomimetic Spn-F alone can activate Rab11. Nevertheless, Rab11 activation downstream of Ik2/Spn-F might still be regulated by inhibiting Rab11 GAPs. To test this possibility, we could promote the activity of Rab11 GAPs candidates by overexpressing them and examine whether there are pruning defects.

Dendrite morphogenesis require positive regulations by Rab11, Parcas, TRAPP complex II, and negative regulations by Crag

Rab11, *pcs* and *brun* mutant larval neurons showed reduced dendrite branching and outgrowth (Fig 2, 4), indicating that Rab11 could be activated by Parcas and TRAPP complex II to positively regulate dendrite morphogenesis. Conversely, *Crag* mutant larval neurons showed exacerbated dendrite branching and outgrowth (Fig 4), which suggests that Crag could be a negative regulator for dendrite morphogenesis. It seems contradictory that Rab11 and Crag, one of the Rab11 GEFs, play opposite roles in dendrite morphogenesis. One possibility is that Rab11 could positively regulate dendrite morphogenesis through Parcas and TRAPP complex II, and also negatively regulate



dendrite morphogenesis through Crag. The other possibility is that Crag regulates dendrite morphogenesis by serving as a Rab10 GEF (Xiong et al., 2012), not as a Rab11 GEF, since Rab10 has been found important for regulating neurite outgrowth in PC12 cells (Homma & Fukuda, 2016) and dendritic branching of PVD sensory neurons in *C. elegans* (Caitlin et al., 2015) (Zou et al., 2015). Last but not least, Crag could regulate dendrite morphogenesis in a GEF-activity-independent manner, as there are several GEFs possessing GEF-activity-independent functions (Homma & Fukuda, 2016) (Miller et al., 2013) (Tang et al., 2019). For example, it was found that the re-expression of a GEF-inactive mutant form of Rgnef, a Rho GEF, in Rgnef-null cells enhanced focal adhesion kinase (FAK) activation to the same level as Rgnef-WT re-expression did, revealing a GEF-activity-independent function of Rgnef (Miller et al., 2013).

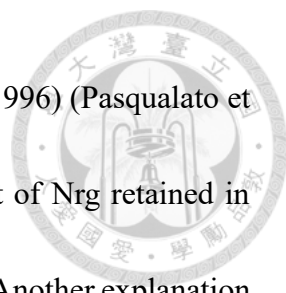
Nrg-internalizing endocytic pathway and potential exocytosis-endocytosis coupling during dendrite pruning

We found that Rab11 perturbation disrupts Rab5-dependent Nrg internalization, which suggests the pruning defects of Rab11 perturbation we observed could be partially contributed by defective Nrg internalization. Another study showed that Arf1-dependent secretory pathway is also required for pruning and proper Nrg degradation (Wang et al.,

2017). This finding raises a possibility that the Rab11- and Arf1-dependent secretory pathway could act coordinately during dendrite pruning.



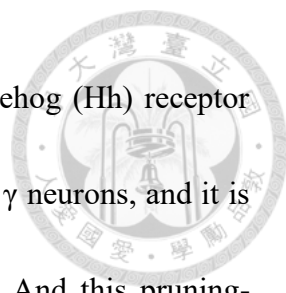
There was a recent study pointing out the role of Rab11 in degradation of not only Nrg but also ion channel Ppk26 in dendrite pruning. They also found that Rab11 is required for the proper localization of these two membrane proteins in larval stage. To be more specific, their finding suggest that some Nrg is retained in recycling endosomes in larval stage without affecting the amount of Nrg on plasma membrane when knocking down Rab11 (Krämer et al., 2019). This seems to be in contradiction with our findings that more Nrg is localized to the somatic plasma membrane in *Rab11* RNAi neurons during white pupal stage (Fig 6J), at which somatic membrane-bound Nrg degradation has not begun (Zhang et al., 2014). To explain this, the notion of coupling between exocytosis and endocytosis should be taken into consideration. In some excitable cells, such as neurons and endocrine cells, localized exocytosis is triggered by membrane depolarization and coupled endocytosis is required to maintain the balance of surface membrane and the pool of vesicles (Liang et al., 2017) (Lou, 2018). Enlightened by this notion, we hypothesize that temporally elevated exocytosis could be a prerequisite for the Nrg-internalizing endocytic pathway in *ddaC* neurons of early pupae. This hypothesis could thereby explain the phenotypes observed in *Rab11* RNAi neurons, whose Nrg might be transported onto somatic membrane at white pupal stage (Fig 6J), even though



recycling is commonly inhibited by Rab11 depletion (Ullrich et al., 1996) (Pasqualato et al., 2004) (Takahashi et al., 2012), since there is significant amount of Nrg retained in recycling endosomes at the first place in larvae (Krämer et al., 2019). Another explanation for the contradictory observation of Nrg localization is that the endocytic rate required for maintaining the amount of somatic membrane-bound Nrg in equilibrium may be higher in white pupae than in larvae. Thus, the potential reduction of endocytic rate in *Rab11* RNAi neurons (Fig 5) could lead to their higher level of Nrg retained on the somatic membrane at white pupal stage (Fig 6J).

The importance of membrane protein degradation in axon and dendrite pruning


Unlike dendrite pruning, Rab11 is not required for axon pruning in mushroom body (MB) γ neurons (Issman-Zecharya & Schuldiner, 2014) and Nrg undergoes little or no endocytosis in those neurons (Zhang et al., 2014). This indicates that Nrg internalization could be a specific requirement for dendrite pruning in ddaC neurons. To elaborate on this, we conjecture that the Nrg internalization during dendrite pruning would lead to loss of dendrite stability, as Nrg has been found to facilitate stabilization of the dendrite-epidermis interface in da neurons (Yang et al., 2019). And the loss of neurite stability is either required specifically in dendrite pruning of ddaC neurons, or mediated by internalizing other cell adhesion molecules in axon pruning.



Nonetheless, it has been found that a membrane protein, Hedgehog (Hh) receptor Patched (Ptc), serves as an inhibitory signal in axon pruning of MB γ neurons, and it is downregulated through ESCRT-dependent endolysosomal pathway. And this pruning-inhibitory role of Ptc is independent of canonical Hedgehog signaling. However, since the ligand-binding domain of Ptc is required for its pruning-inhibitory function (Issman-Zecharya & Schuldiner, 2014), there could be ligands other than Hh facilitating inhibition of pruning through Ptc. With regards to this, Ptc was also found to function as a lipoprotein receptor (Callejo et al., 2008).

Potential role of Rab11 in varicosities formation during dendrite pruning

Rab11 is localized on TGN, post-Golgi vesicles and pericentriolar recycling endosomes to mediate exocytic or recycling processes (Welz et al., 2014). These exocytic/recycling processes are required for transporting proteins or membrane to the cell surface, so we could therefore draw a simple inference that either some unknown molecules or membranes need to be transported onto cell surface through Rab11-dependent trafficking during dendrite pruning. With that being said, there is indeed a membranous structural change in proximal dendrites prior to pruning. Specifically, there are membranous bulges called varicosities formed at proximal dendrites next to dendritic thinning sites, where dendrites are destined to be severed, from 3h APF. It will be

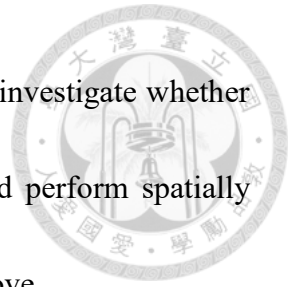


intriguing to examine whether Rab11 regulates locally enhanced exocytic activity to promote these varicosities formation. Furthermore, it will also be interesting to investigate how varicosities formation coordinate with dendritic thinning, which requires locally enhanced Rab5-dependent endocytic activity (Kanamori et al., 2015).

Spn-F may serve as a platform for linking Rab11 and Dynein motor complex to mediate transportation of Rab11 on dendrites

In this study, we pointed out the SCD domain in Spn-F is to mediate interaction with Rab11. Previously, we have also found that the SCD domain is required for interacting with Cut up (Ctp), the *Drosophila* homologue of Dynein light chain 1 (Lin et al., 2015). Since Spn-F interacts with both Rab11 and Dynein complex through SCD domain, it could be the linkage between Rab11 and Dynein motor complex. Regarding this, Spn-F puncta undergo Dynein-dependent dispersion after being phosphorylated by Ik2 kinase in early pupae (Lin et al., 2015); however, the destination of dispersed Spn-F is unknown. Dynein is one of the microtubules (MTs) motor protein and it moves on MTs toward their minus ends. MTs are mainly oriented minus-ends-out in proximal dendrites of *Drosophila* neurons (Stone et al., 2008), so Dynein may transport Spn-F and Rab11 to the proximal dendrites of ddaC neurons. To support this notion, there has been found that the Spn-F puncta in *Drosophila* nurse cells undergo Dynein-dependent dispersion towards minus

ends of MTs in oocytes (Abdu et al., 2006). It will be interesting to investigate whether Rab11 and Spn-F are indeed transported to proximal dendrites and perform spatially regulated functions, such as the varicosities formation mentioned above.



Ik2-regulated recycling endosome shuttling

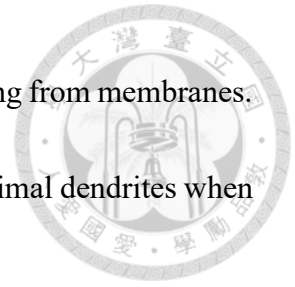
The function of Spn-F we proposed above is reminiscent of the role of a Rab11 effector, Nuclear fallout (Nuf), in bristle elongation. Nuf interacts with Rab11 and Dynein light intermediate chain (Horgan et al., 2010) and moves along MTs toward distal end of bristles, where the MT minus ends oriented (Bitan et al., 2010), during bristle elongation. When transported to bristle tips, Nuf is phosphorylated by Ik2 to promote recycling endosomes shuttling (Otani et al., 2011).

Being a substrate for Ik2 and interacting partners for both Rab11 and Dynein, Spn-F could share similarities with Nuf in regulating transportation of recycling endosomes towards MT minus ends. However, our finding (by Dr. T. Ln) that Spn-F associates more strongly with Rab11 GDP-bound form than with GTP-bound form suggests that Spn-F might transport Rab11 molecules, not Rab11-positive vesicles, since the GDP-bound form of Rab proteins is considered to be soluble in cytosol (Zhen & Stenmark, 2015). Nevertheless, the GDP-bound form human Rab11a has been proposed to associate with membrane based on crystallographic studies (Pasqualato et al., 2004), opening the

possibility that Rab11 undergoes GTP/GDP cycles without dissociating from membranes.

Thus, Spn-F may transport Rab11-GDP-bound vesicles towards proximal dendrites when

being phosphorylated by Ik2 prior to pruning.



Reference



Abdu U, Bar D, Schüpbach T. (2006) spn-F encodes a novel protein that affects oocyte patterning and bristle morphology in *Drosophila*. *Development* 133(8):1477-84.

Ainsley JA, Pettus JM, Bosenko D. (2003) Enhanced locomotion caused by loss of the *Drosophila* DEG/ENaC protein Pickpocket1. *Curr Biol* 13(17): 1557--1563.

Bagri A, Cheng HJ, Yaron A, Pleasure SJ, Tessier-Lavigne M. (2003) Stereotyped pruning of long hippocampal axon branches triggered by retraction inducers of the semaphorin family. *Cell* 113(3):285-99.

Barr F, Lambright DG. (2010) Rab GEFs and GAPs. *Curr Opin Cell Biol* 22(4):461-70.

Bitan A, Guild GM, Bar-Dubin D, Abdu U. (2010) Asymmetric microtubule function is an essential requirement for polarized organization of the *Drosophila* bristle. *Mol Cell Biol* 30(2):496-507.

Bogard N, Lan L, Xu J, Cohen RS. (2007) Rab11 maintains connections between germline stem cells and niche cells in the *Drosophila* ovary. *Development* 134(19):3413-8.

Callejo A, Culi J, Guerrero I. (2008) Patched, the receptor of Hedgehog, is a lipoprotein receptor. *Proc Natl Acad Sci U S A* 105(3):912-917.

Cocchi E, Drago A, Serretti A. (2016) Hippocampal Pruning as a New Theory of Schizophrenia Etiopathogenesis. *Mol Neurobiol* 53(3):2065-2081.

Consoulas C, Duch C, Bayline RJ, Levine RB. (2000) Behavioral transformations during metamorphosis: remodeling of neural and motor systems. *Brain Res Bull* 53(5):571-83.

Cowan WM, Fawcett JW, O'Leary DD, Stanfield BB. (1984) Regressive events in neurogenesis. *Science* 225(4668):1258-65.

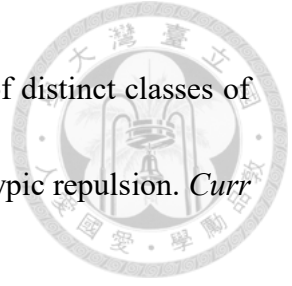
Dubin-Bar D, Bitan A, Bakhrat A, Kaiden-Hasson R, Etzion S, Shaanan B, Abdu U. (2008) The *Drosophila* IKK-related kinase (Ik2) and Spindle-F proteins are part of a complex that regulates cytoskeleton organization during oogenesis. *BMC Cell Biol* 9:51.

Ferreira T, Blackman A, Oyrer J, Jayabal A, Chung A, Watt A, Sjöström J and van Meyel D (2014). Neuronal morphometry directly from bitmap images. *Nat Methods* 11(10): 982–984.

Fortier E, Belote JM. (2000) Temperature-dependent gene silencing by an expressed inverted repeat in *Drosophila*. *Genesis* 26(4):240-4.

Gillooly DJ, Morrow IC, Lindsay M, Gould R, Bryant NJ, Gaullier JM, Parton RG, Stenmark H. (2000) Localization of phosphatidylinositol 3-phosphate in yeast and mammalian cells. *EMBO J* 19(17):4577-88.

Goody RS, Müller MP, Wu YW. (2017) Mechanisms of action of Rab proteins, key regulators of intracellular vesicular transport. *Biol Chem* 398(5-6):565-575.



Grueber WB, Ye B, Moore AW, Jan LY, Jan YN. (2003) Dendrites of distinct classes of *Drosophila* sensory neurons show different capacities for homotypic repulsion. *Curr Biol* 13(8):618-26.

Grueber WB, Ye B, Yang CH, Younger S, Borden K, Jan LY, Jan YN. (2007) Projections of *Drosophila* multidendritic neurons in the central nervous system: links with peripheral dendrite morphology. *Development* 134(1):55-64.

Han C, Song Y, Xiao H, Wang D, Franc NC, Jan LY, Jan YN. (2014) Epidermal cells are the primary phagocytes in the fragmentation and clearance of degenerating dendrites in *Drosophila*. *Neuron* 81(3):544-560.

Homma Y, Fukuda M. (2016) Rabin8 regulates neurite outgrowth in both GEF activity-dependent and -independent manners. *Mol Biol Cell* 27(13):2107-18.

Horgan CP, Hanscom SR, Jolly RS, Futter CE, McCaffrey MW. (2010) Rab11-FIP3 links the Rab11 GTPase and cytoplasmic dynein to mediate transport to the endosomal-recycling compartment. *J Cell Sci* 123(Pt 2):181-91.

Innocenti GM, Price DJ. (2005) Exuberance in the development of cortical networks. *Nat Rev Neurosci* 6(12):955-65.

Issman-Zecharya N, Schuldiner O. (2014) The PI3K class III complex promotes axon pruning by downregulating a Ptc-derived signal via endosome-lysosomal degradation. *Dev Cell* 31(4):461-73.

Takegawa W, Mitakidis N, Miura E, Abe M, Matsuda K, Takeo YH, Kohda K, Motohashi

J, Takahashi A, Nagao S, Muramatsu S, Watanabe M, Sakimura K, Aricescu AR,

Yuzaki M. (2015) Anterograde C1ql1 signaling is required in order to determine and

maintain a single-winner climbing fiber in the mouse cerebellum. *Neuron* 85(2):316-

29.

Kanamori T, Kanai MI, Dairyo Y, Yasunaga K, Morikawa RK, Emoto K. (2013)

Compartmentalized calcium transients trigger dendrite pruning in *Drosophila*

sensory neurons. *Science* 340(6139):1475-8.

Kanamori T, Yoshino J, Yasunaga K, Dairyo Y, Emoto K. (2015) Local endocytosis

triggers dendritic thinning and pruning in *Drosophila* sensory neurons. *Nat Commun*

6:6515.

Kirilly D, Gu Y, Huang Y, Wu Z, Bashirullah A, Low BC, Kolodkin AL, Wang H, Yu F.

(2009) A genetic pathway composed of Sox14 and Mical governs severing of

dendrites during pruning. *Nat Neurosci* 12(12):1497–505.

Kuo CT, Jan LY, Jan YN. (2005) Dendrite-specific remodeling of *Drosophila* sensory

neurons requires matrix metalloproteases, ubiquitin-proteasome, and ecdysone

signaling. *Proc Natl Acad Sci U S A* 102(42):15230–5.

Kuo CT, Zhu S, Younger S, Jan LY, Jan YN. (2006) Identification of E2/E3 ubiquitinating enzymes and caspase activity regulating *Drosophila* sensory neuron dendrite pruning. *Neuron* 51(3):283–90.

Kuranaga E, Kanuka H, Tonoki A, Takemoto K, Tomioka T, Kobayashi M, Hayashi S, Miura M. (2006) *Drosophila* IKK-related kinase regulates nonapoptotic function of caspases via degradation of IAPs. *Cell* 126(3):583-96.

Lee HH, Jan LY, Jan YN. (2009) *Drosophila* IKK-related kinase Ik2 and Katanin p60-like 1 regulate dendrite pruning of sensory neuron during metamorphosis. *Proc Natl Acad Sci U S A* 106(15):6363–8.

Lee T, Luo L. (1999) Mosaic analysis with a repressible cell marker for studies of gene function in neuronal morphogenesis. *Neuron* 22(3):451-61.

Lee T, Marticke S, Sung C, Robinow S, Luo L. (2000) Cell-autonomous requirement of the USP/EcR-B ecdysone receptor for mushroom body neuronal remodeling in *Drosophila*. *Neuron* 28(3):807-18.

Liang K, Wei L, Chen L. (2017) Exocytosis, Endocytosis, and Their Coupling in Excitable Cells. *Front Mol Neurosci* 10:109.

Lin T, Pan PY, Lai YT, Chiang KW, Hsieh HL, Wu YP, Ke JM, Lee MC, Liao SS, Shih HT, Tang CY, Yang SB, Cheng HC, Wu JT, Jan YN, Lee HH. (2015) Spindle-F Is the



Central Mediator of Ik2 Kinase-Dependent Dendrite Pruning in *Drosophila* Sensory Neurons. *PLoS Genet* 11(11):e1005642.

Loncle N, Williams DW. (2012) An interaction screen identifies headcase as a regulator of large-scale pruning. *J Neurosci* 32(48):17086-96.

Lou X. (2018) Sensing Exocytosis and Triggering Endocytosis at Synapses: Synaptic Vesicle Exocytosis-Endocytosis Coupling. *Front Cell Neurosci* 12:66.

Mani R, St Onge RP, Hartman JL 4th, Giaever G, Roth FP. (2008) Defining genetic interaction. *Proc Natl Acad Sci U S A* 105(9):3461-6.

Marin EC, Watts RJ, Tanaka NK, Ito K, Luo L. (2005) Developmentally programmed remodeling of the *Drosophila* olfactory circuit. *Development* 132(4):725-37.

Miller NL, Lawson C, Kleinschmidt EG, Tancioni I, Uryu S, Schlaepfer DD. (2013) A non-canonical role for Rgnef in promoting integrin-stimulated focal adhesion kinase activation. *J Cell Sci* 126(Pt 21):5074-85

Nicholson L, Singh GK, Osterwalder T, Roman GW, Davis RL, Keshishian H. (2008) Spatial and temporal control of gene expression in *Drosophila* using the inducible GeneSwitch GAL4 system. I. Screen for larval nervous system drivers. *Genetics* 178(1):215-34.

Otani T, Oshima K, Onishi S, Takeda M, Shinmyozu K, Yonemura S, Hayashi S. (2011)

IKK ϵ regulates cell elongation through recycling endosome shuttling. *Dev Cell* 20(2):219-32.

Pasqualato S, Senic-Matuglia F, Renault L, Goud B, Salamero J, Cherfils J. (2004) The structural GDP/GTP cycle of Rab11 reveals a novel interface involved in the dynamics of recycling endosomes. *J Biol Chem* 279(12):11480-8.

Riedel F, Galindo A, Muschalik N, Munro S. (2018) The two TRAPP complexes of metazoans have distinct roles and act on different Rab GTPases. *J Cell Biol* 217(2):601-617.

Rouw R, Scholte HS. (2007) Increased structural connectivity in grapheme-color synesthesia. *Nat Neurosci* 10(6):792-7.

Schindelin J, Arganda-Carreras I, Frise E, Kaynig V, Longair M, Pietzsch T, Preibisch S, Rueden C, Saalfeld S, Schmid B, Tinevez JY, White DJ, Hartenstein V, Eliceiri K, Tomancak P, Cardona A. (2012) Fiji: an open-source platform for biological-image analysis. *Nat Methods* 9(7): 676–682.

Schuldiner O, Yaron A. (2015) Mechanisms of developmental neurite pruning. *Cell Mol Life Sci* 72(1):101-19.

Shapiro RS, Anderson KV. (2006) *Drosophila* Ik2, a member of the I kappa B kinase family, is required for mRNA localization during oogenesis. *Development* 133(8):1467-75.



Singh AP, VijayRaghavan K, Rodrigues V. (2010) Dendritic refinement of an identified neuron in the *Drosophila* CNS is regulated by neuronal activity and Wnt signaling. *Development* 137(8):1351-60.

Stenmark H, Parton RG, Steele-Mortimer O, Lütcke A, Gruenberg J, Zerial M. (1994) Inhibition of rab5 GTPase activity stimulates membrane fusion in endocytosis. *EMBO J* 13(6):1287–1296.

Stone MC, Roegiers F, Rolls MM. (2008) Microtubules have opposite orientation in axons and dendrites of *Drosophila* neurons. *Mol Biol Cell* 19(10):4122-9.

Takahashi S, Kubo K, Waguri S, Yabashi A, Shin HW, Katoh Y, Nakayama K. (2012) Rab11 regulates exocytosis of recycling vesicles at the plasma membrane. *J Cell Sci* 125(Pt 17):4049-57.

Tang G, Gudsruk K, Kuo SH, Cotrina ML, Rosoklija G, Sosunov A, Sonders MS, Kanter E, Castagna C, Yamamoto A, Yue Z, Arancio O, Peterson BS, Champagne F, Dwork AJ, Goldman J, Sulzer D. (2014) Loss of mTOR-dependent macroautophagy causes autistic-like synaptic pruning deficits. *Neuron* 83(5):1131-43.

Tang LT, Diaz-Balzac CA, Rahman M, Ramirez-Suarez NJ, Salzberg Y, Lázaro-Peña MI,

Bülow HE. (2019) TIAM-1/GEF can shape somatosensory dendrites independently of its GEF activity by regulating F-actin localization. *Elife* 8. pii: e38949.

Tapia JC, Wylie JD, Kasthuri N, Hayworth KJ, Schalek R, Berger DR, Guatimosim C,

Seung HS, Lichtman JW. (2012) Pervasive synaptic branch removal in the mammalian neuromuscular system at birth. *Neuron* 74(5):816-29.

Taylor CA, Yan J, Howell AS, Dong X, and Shen K. (2015) RAB-10 Regulates Dendritic

Branching by Balancing Dendritic Transport. *PLoS Genet* 11(12):e1005695.

Thompson RA, Nelson CA. (2001) Developmental science and the media. Early brain

development. *Am Psychol* 56(1):5–15.

Ullrich O, Reinsch S, Urbé S, Zerial M, Parton RG. (1996) Rab11 regulates recycling

through the pericentriolar recycling endosome. *J Cell Biol* 135(4):913-24.

Urbé S, Huber LA, Zerial M, Tooze SA, Parton RG. (1993) Rab11, a small GTPase

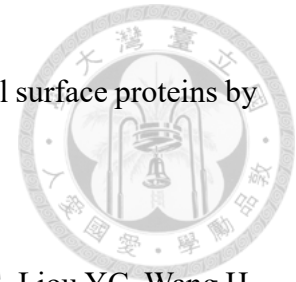
associated with both constitutive and regulated secretory pathways in PC12 cells.

FEBS Lett 334(2):175-82.

Wang Y, Zhang H, Shi M, Liou YC, Lu L, Yu F. (2017) Sec71 functions as a GEF for the

small GTPase Arf1 to govern dendrite pruning of *Drosophila* sensory neurons.

Development 144(10):1851-1862.



Welz T, Wellbourne-Wood J, Kerkhoff E. (2014) Orchestration of cell surface proteins by Rab11. *Trends Cell Biol* 24(7):407-15.

Wong JJ, Li S, Lim EK, Wang Y, Wang C, Zhang H, Kirilly D, Wu C, Liou YC, Wang H, Yu F. (2013) A Cullin1-based SCF E3 ubiquitin ligase targets the InR/PI3K/TOR pathway to regulate neuronal pruning. *PLoS Biol* 11(9):e1001657.

Xiong B, Bayat V, Jaiswal M, Zhang K, Sandoval H, Charng WL, Li T, David G, Duraine L, Lin YQ, Neely GG, Yamamoto S, Bellen HJ. (2012) Crag is a GEF for Rab11 required for rhodopsin trafficking and maintenance of adult photoreceptor cells. *PLoS Biol* 10(12):e1001438.

Yang WK, Chueh YR, Cheng YJ, Siegenthaler D, Pielage J, Chien CT. (2019) Epidermis-Derived L1CAM Homolog Neuroglial Mediates Dendrite Enclosure and Blocks Heteroneuronal Dendrite Bundling. *Curr Biol* 29(9):1445-1459.

Yu F, Schuldiner O. (2014) Axon and dendrite pruning in *Drosophila*. *Curr Opin Neurobiol* 27:192-8.

Zhang H, Wang Y, Wong JJ, Lim KL, Liou YC, Wang H, Yu F. (2014) Endocytic pathways downregulate the L1-type cell adhesion molecule neuroglial to promote dendrite pruning in *Drosophila*. *Dev Cell* 30(4):463-78.

Zhang J, Schulze KL, Hiesinger PR, Suyama K, Wang S, Fish M, Acar M, Hoskins RA,

Bellen HJ, Scott MP. (2007) Thirty-one flavors of *Drosophila* rab proteins. *Genetics*

176(2):1307-22.

Zhen Y, Stenmark H. (2015) Cellular functions of Rab GTPases at a glance. *J Cell Sci*

128(17):3171-6.

Zhu S, Chen R, Soba P, Jan YN. (2019) JNK signaling coordinates with ecdysone

signaling to promote pruning of *Drosophila* sensory neuron dendrites. *Development*

146(8).

Zou W, Yadav S, DeVault L, Nung Jan Y, Sherwood DR. (2015) RAB-10-Dependent

Membrane Transport Is Required for Dendrite Arborization. *PLoS Genet*

11(9):e1005484.

Figure 1

Pupae (16 h APF)

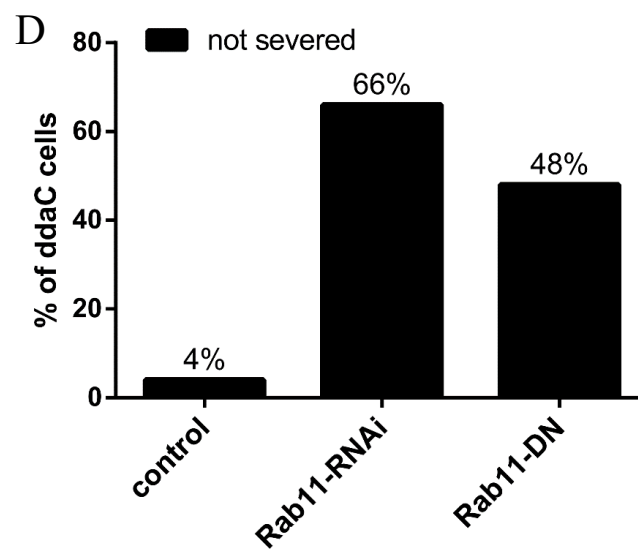
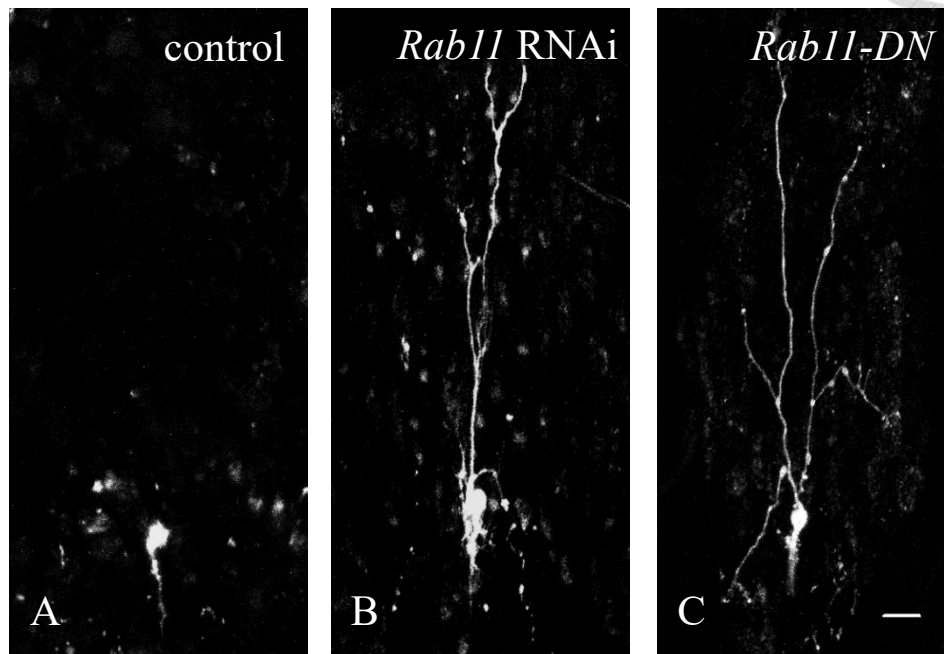


Figure 1. Rab11 GTPase is required for dendrite pruning in ddaC neurons.

(A-C) The ddaC neurons were specifically labeled with *ppk-CD4-tdTomato*. At 16h APF, the dendrites were normally pruned in control neurons (A), but still attached to soma in neurons expressing *Rab11-dsRNA* (B) and Rab11-DN (C). (D) Quantitative analysis of pruning phenotypes at 16h APF in control neurons, neurons with *Rab11-RNAi* and Rab11-DN expression. The percentage of ddaC cells stands for the ratio of the number of neurons with unsevered dendrites to the total number of neurons examined. The number of neurons examined was as follows: for control, n=100; for *Rab11-dsRNA*, n=110; for *Rab11-DN*, n=120. Scale bar, 20 μ m.

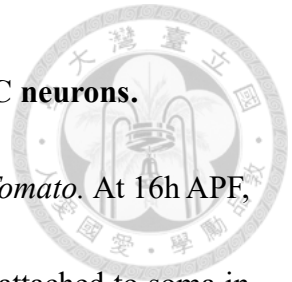
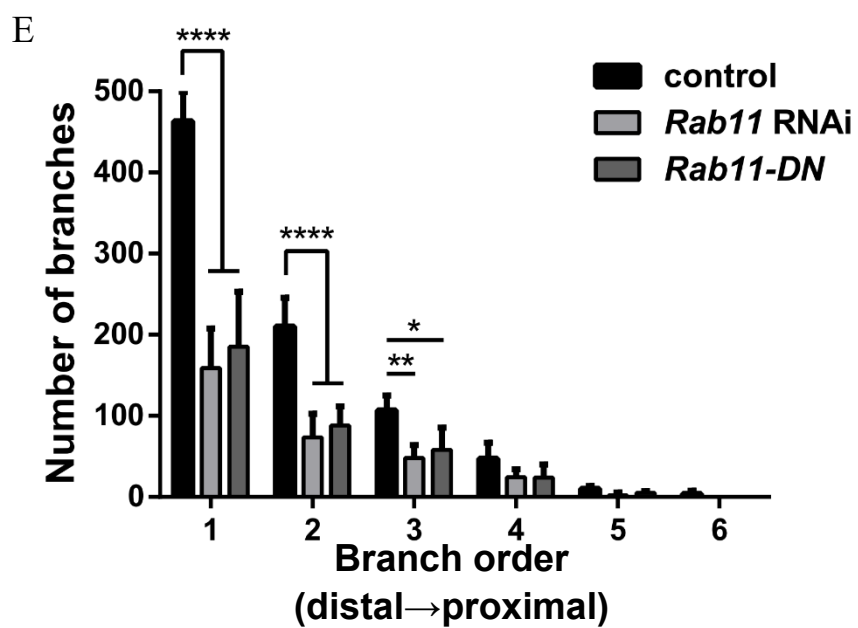
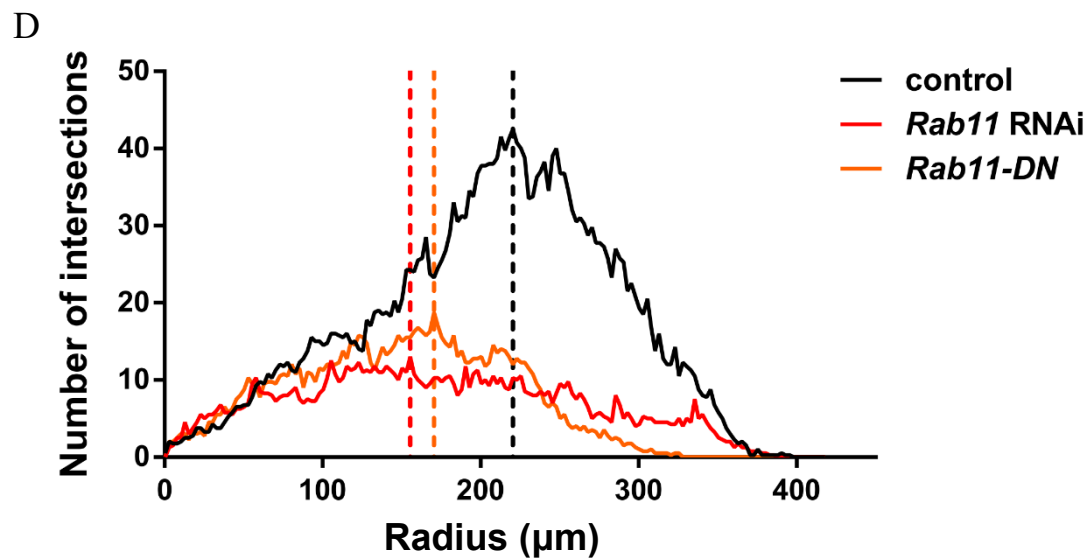
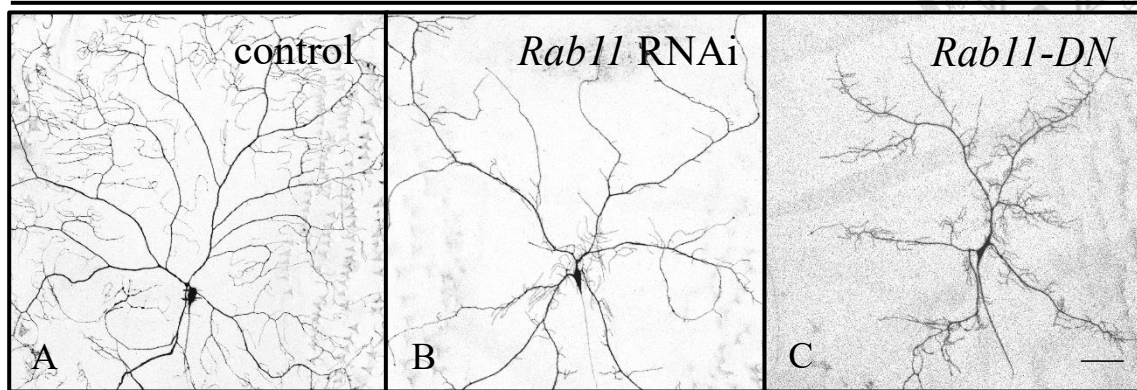


Figure 2

Third instar larvae



F

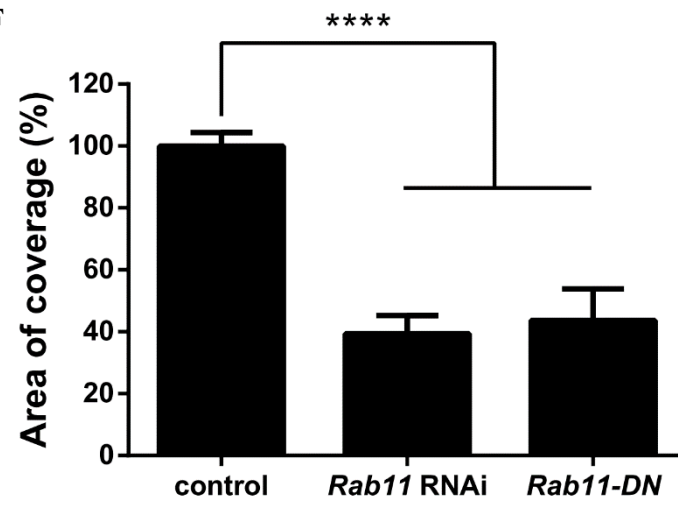


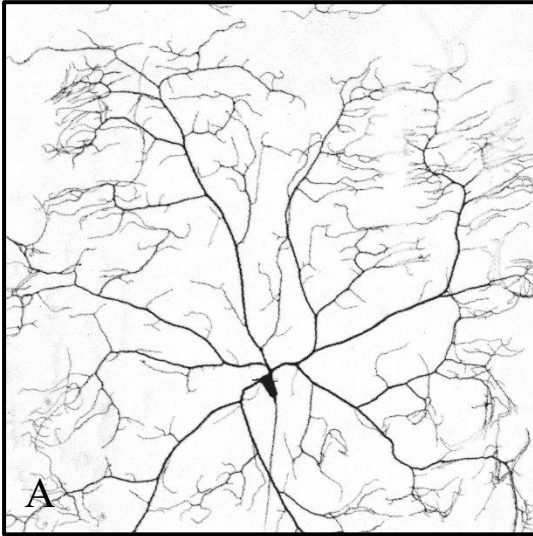
Figure 2. Rab11 is crucial for dendrite morphogenesis in ddaC neurons.

(A, B) The ddaC neurons were marked by *ppk-CD4-tdTomato*. (C) The ddaC neurons were visualized by *ppk-GAL4* and *UAS-mCD8GFP*. In larvae, the control neurons showed normal dendrite morphology and tiling (A), whereas in the neurons with *Rab11-dsRNA* (B) or Rab11-DN (C) expression, there were fewer terminal dendrites and less area of coverage. The number of neurons examined was as follows: for control, n=50; for *Rab11-dsRNA*, n=50; for *Rab11-DN*, n=60. Sholl analysis (D) and Strahler analysis (E) were performed to measure dendritic branching complexity in control neurons, *Rab11* RNAi neurons, and Rab11-DN-expressing neurons. The curve in Sholl analysis was plotted by average number of intersections. The dashed lines in (D) represent the radius with maximal intersections. (F) The percentage of area of dendritic coverage was calculated from dividing the dendritic area of Rab11 mutant neurons by that of control neurons. Scale bar, 50 μ m.

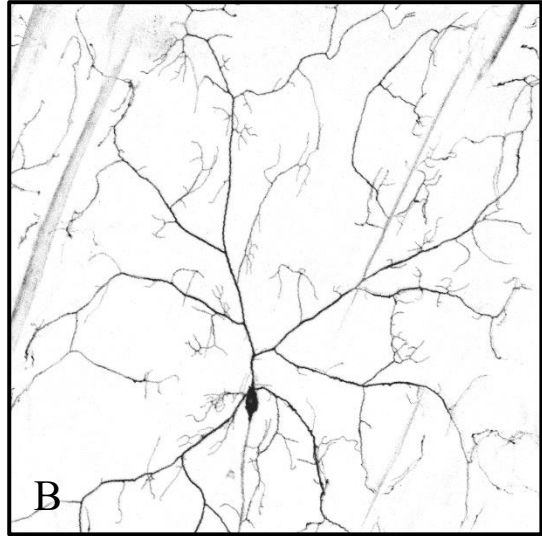
Figure 3

Third instar larvae (GeneSwitch)

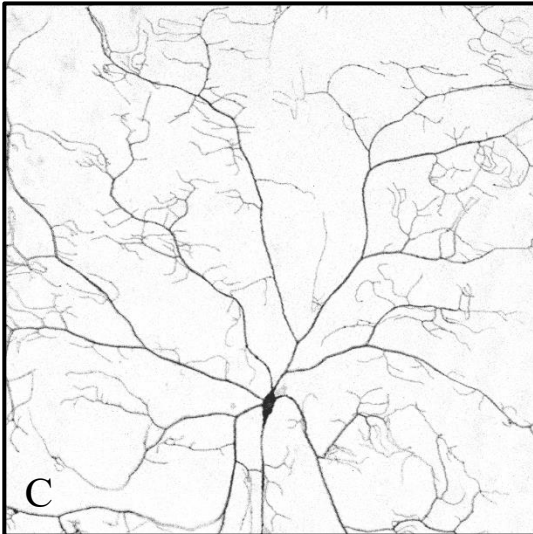
Rab11-DN (non-induced)



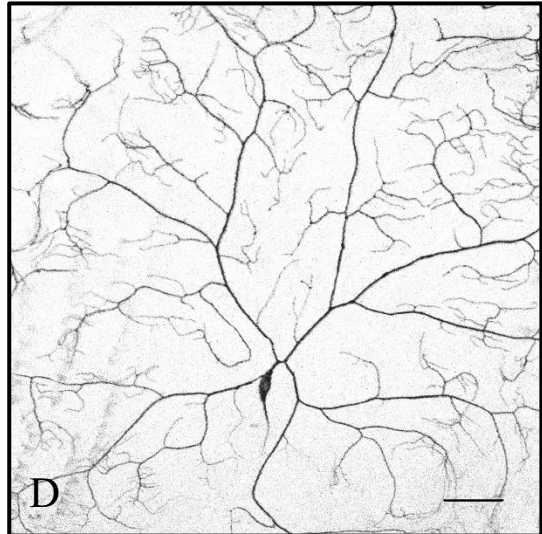
Rab11-DN (induced at 84h AEL)



Rab11-DN (induced at 96h AEL)

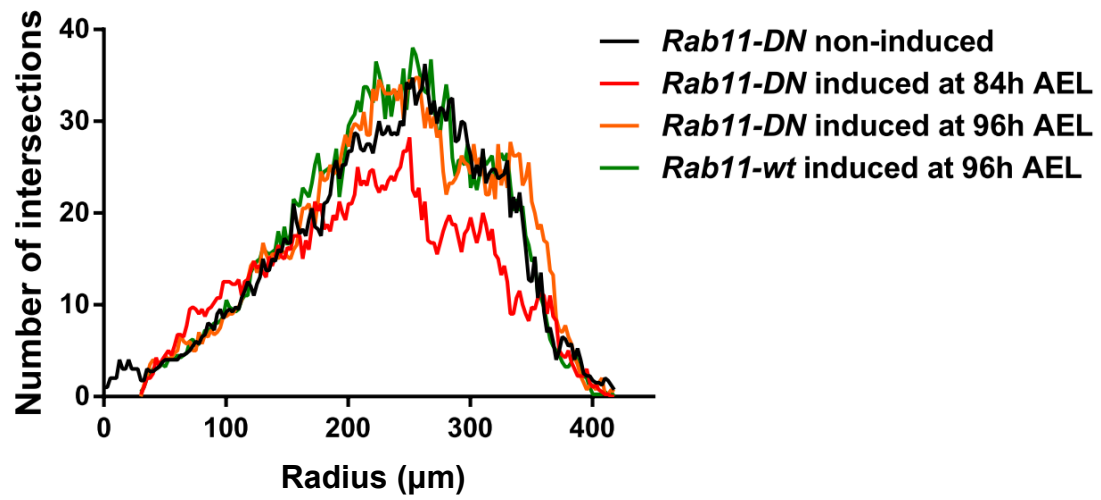


Rab11-wt (induced at 96h AEL)

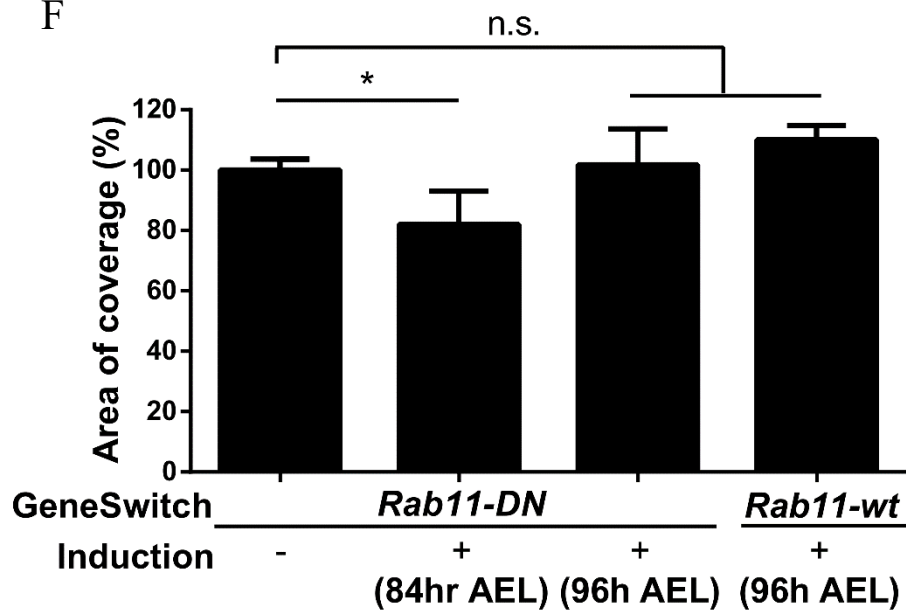




E



F



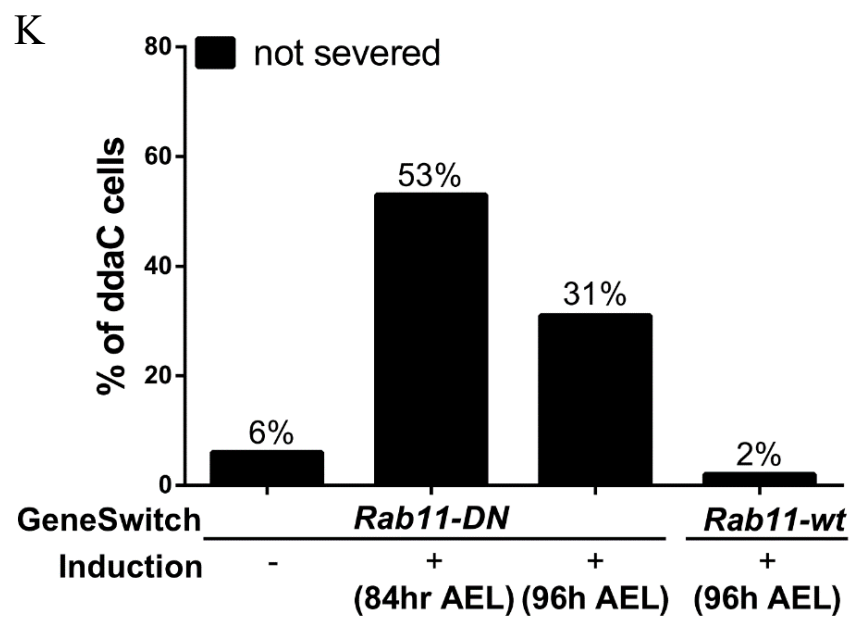
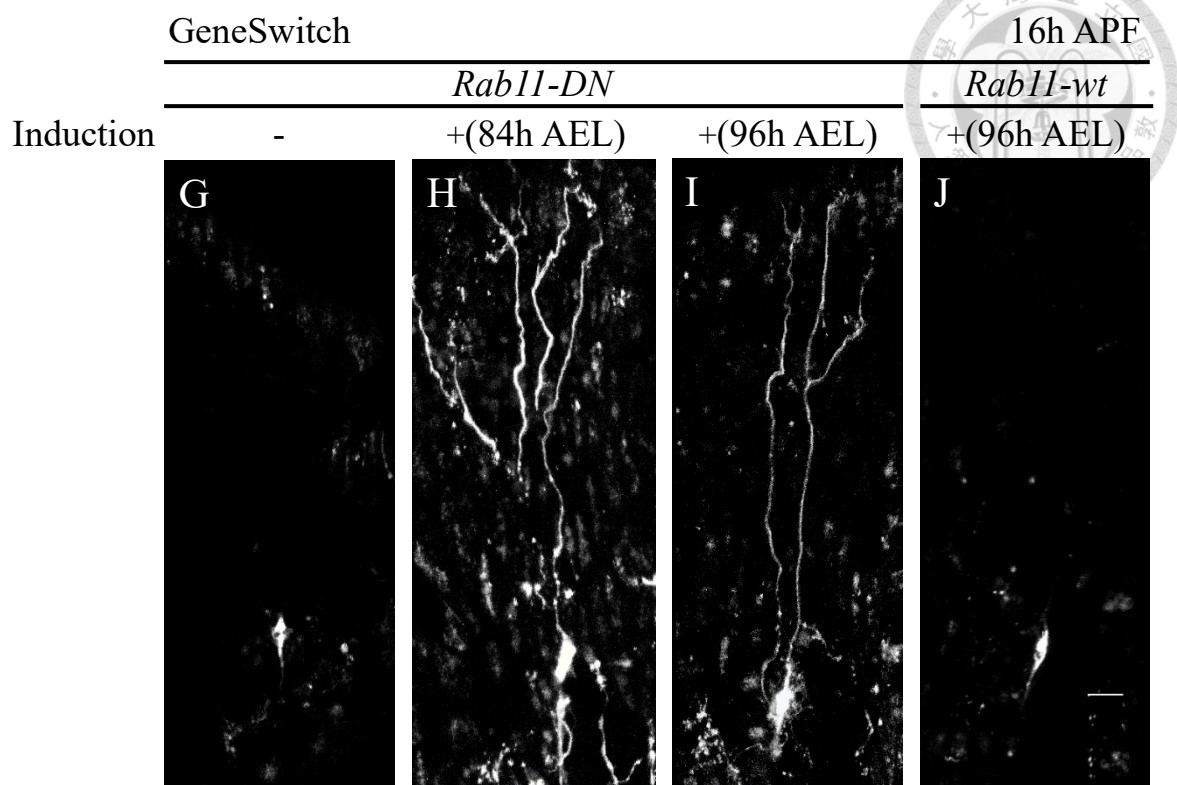


Figure 3. Rab11 is indeed required for dendrite pruning in ddaC neurons.

(A-D) The ddaC neurons were marked by *ppk-CD4-tdTomato*. By utilizing *GSG2295* (GeneSwitch) line, Rab11-DN and Rab11-wt expression could be induced upon RU486 administration. The dendritic morphology of ddaC neurons in larvae without Rab11-DN induction, n=11 (A); larvae with Rab11-DN induction at 84h AEL, n=50 (B); larvae with Rab11-DN induction at 96h AEL, n=80 (C); and larvae with Rab11-wt induction at 96h AEL, n=70 (D). (E) Sholl analysis was executed to measure dendritic branching complexity in these larval neurons. Average number of intersections was plotted. (F) The percentage of area of dendritic coverage was calculated from dividing the dendritic area of larval neurons with transgene induction by that of larval neurons without induction. At 16h APF, the dendrites of neurons without Rab11-DN induction (G) or with Rab11-wt induction at 96h AEL (J) were pruned. After inducing Rab11-DN expression at either 84h or 96h AEL, the dendrites could not be severed properly (H, I). (K) Quantitative analysis of pruning phenotypes at 16h APF in neurons without Rab11-DN induction, neurons with Rab11-DN induction at 84h or 96h AEL, and neurons with Rab11-wt induction at 96h AEL. The percentage of ddaC cells stands for the ratio of the number of neurons with unsevered dendrites to the total number of neurons examined in each condition. The number of neurons examined was as follows: for Rab11-DN non-induction and Rab11-

DN induction at 96h AEL, n=110; for Rab11-DN induction at 84h AEL, n=80; for Rab11-wt induction at 96h AEL, n=90. Scale bar, 50 μ m in (D); 20 μ m in (H).

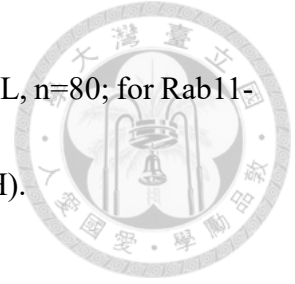
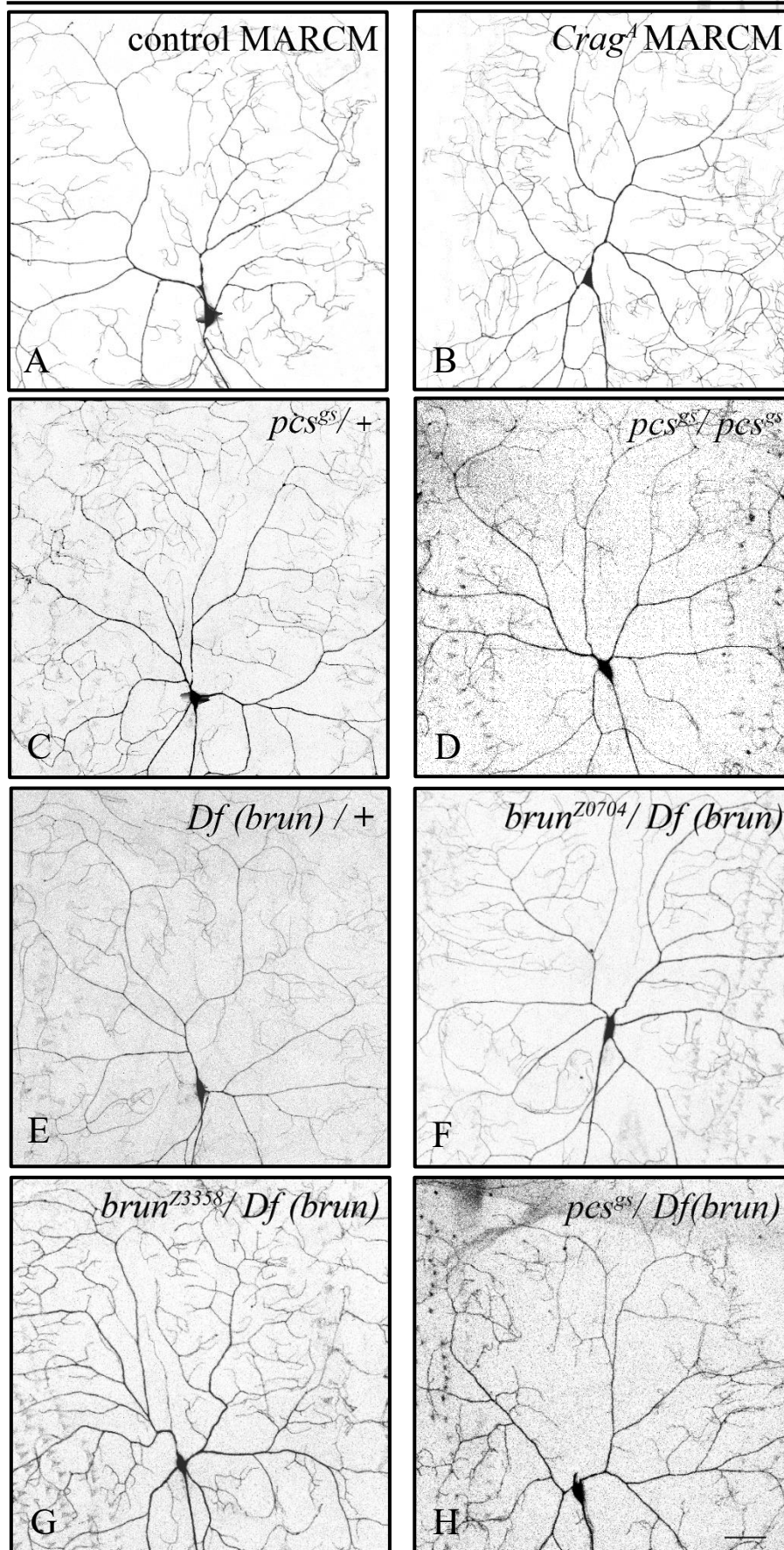
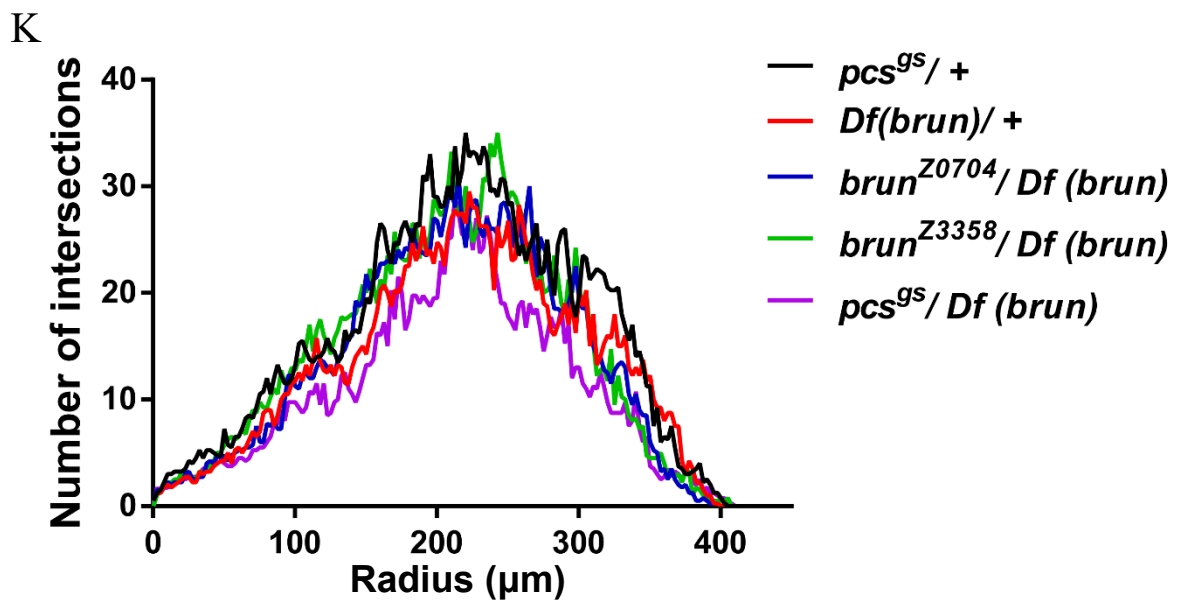
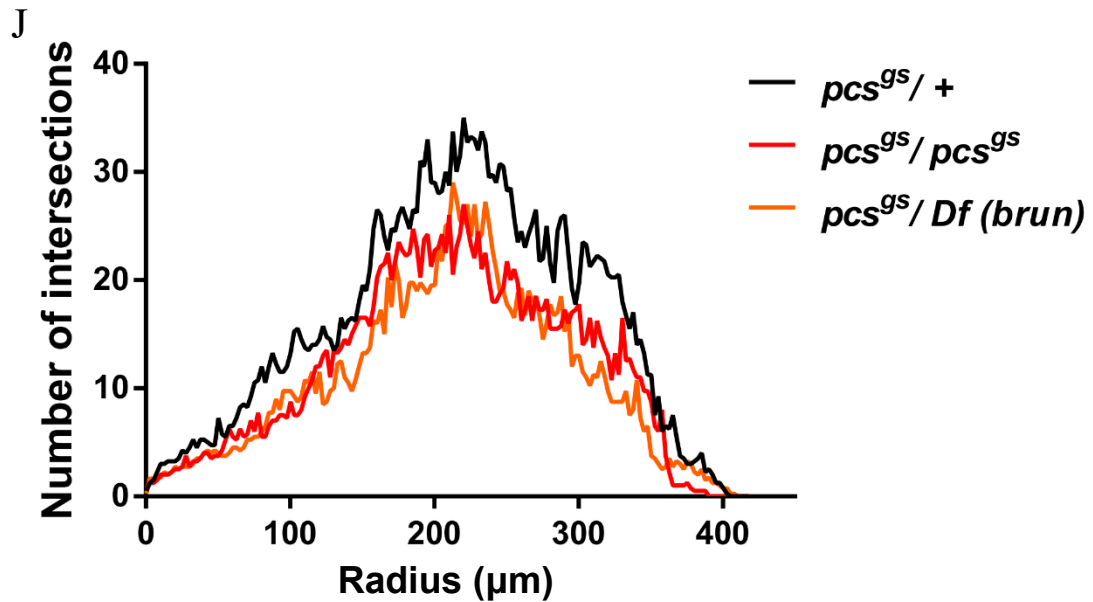
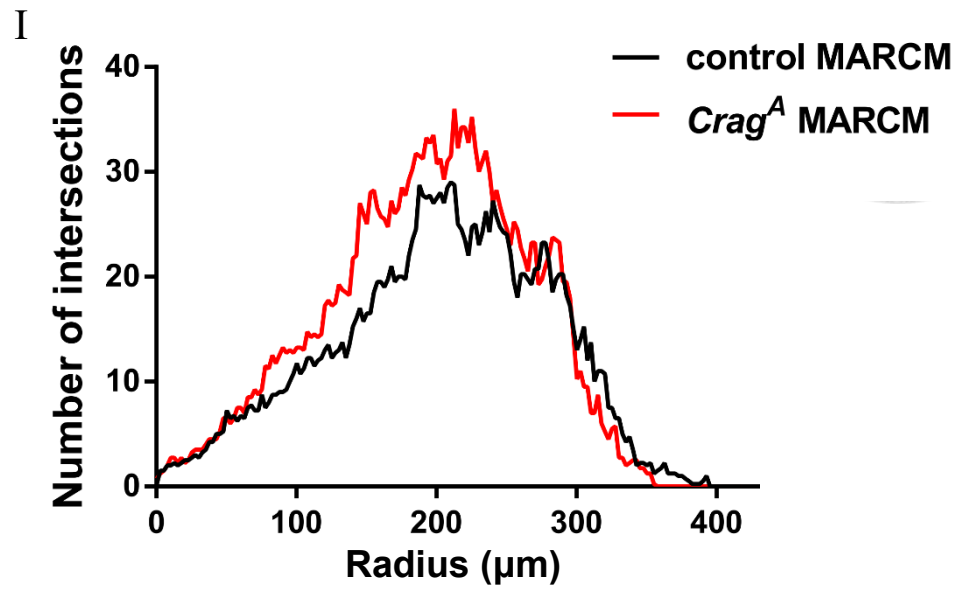
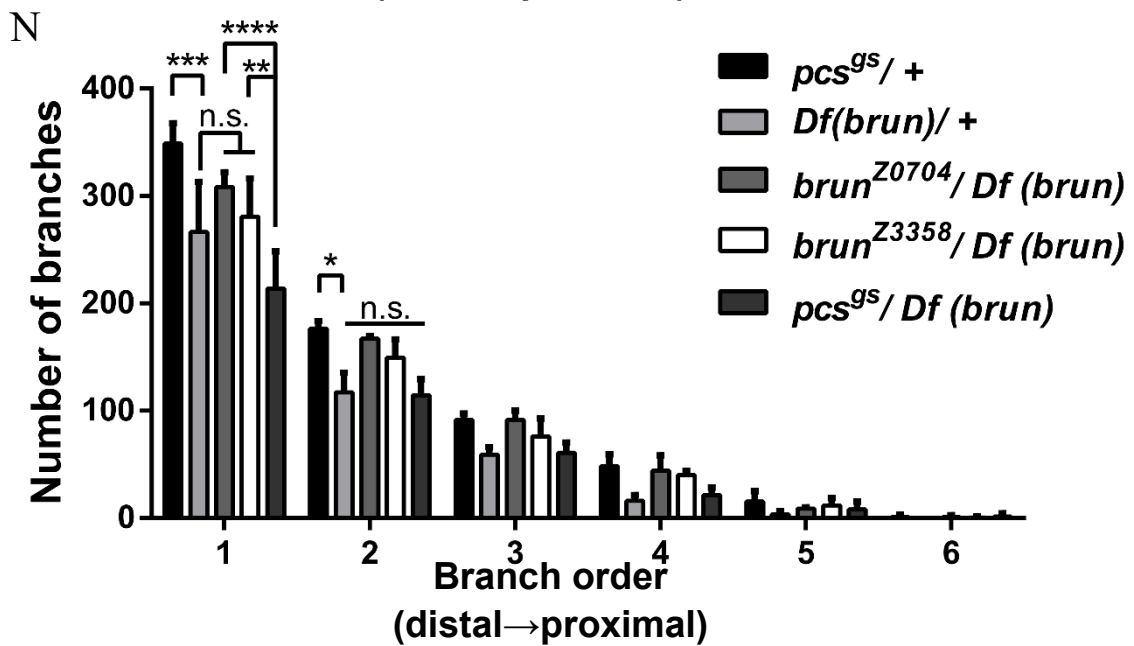
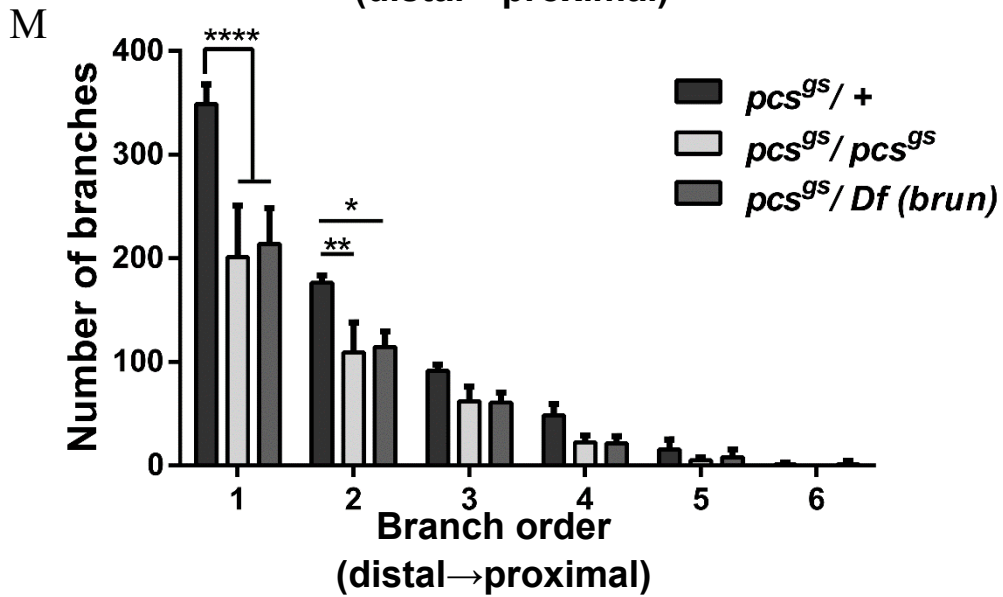
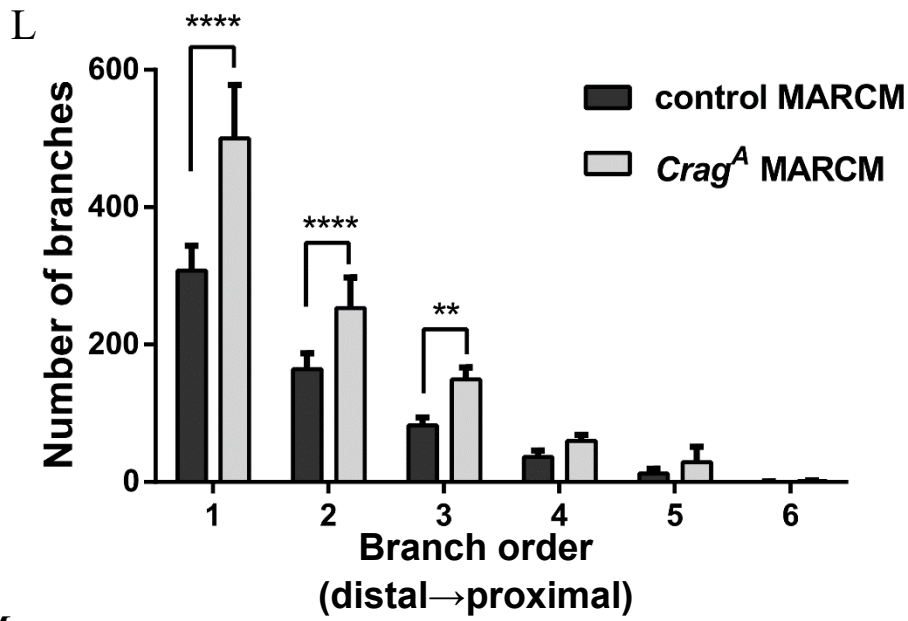


Figure 4

Third instar larvae

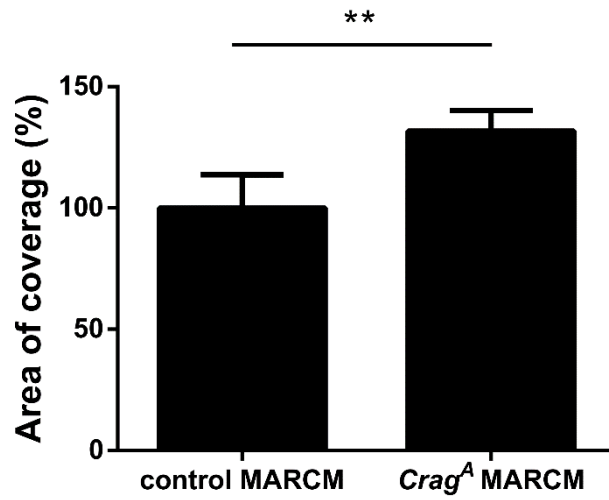




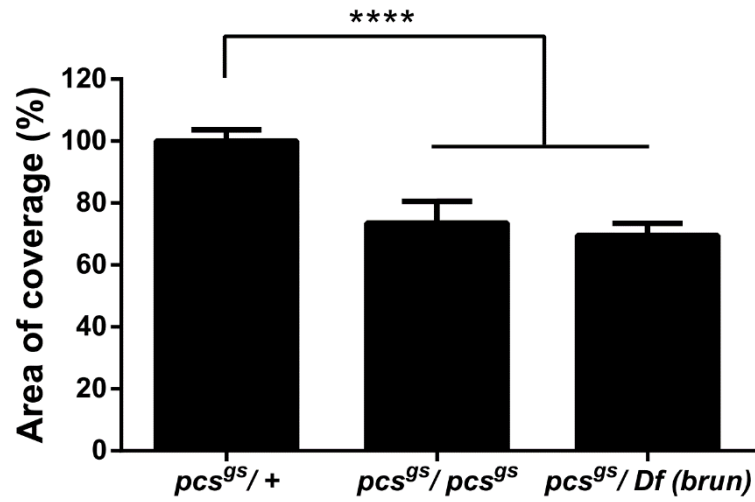




O



P



Q

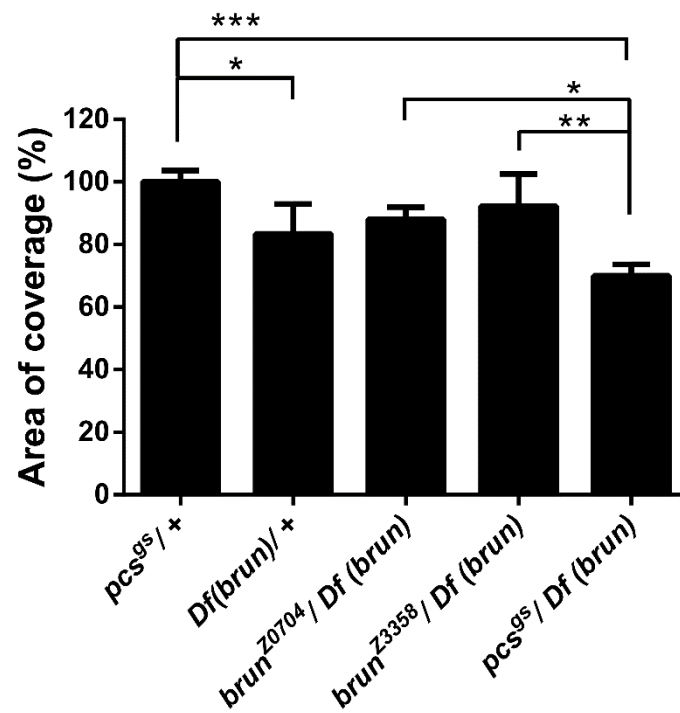
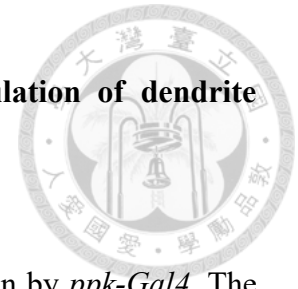
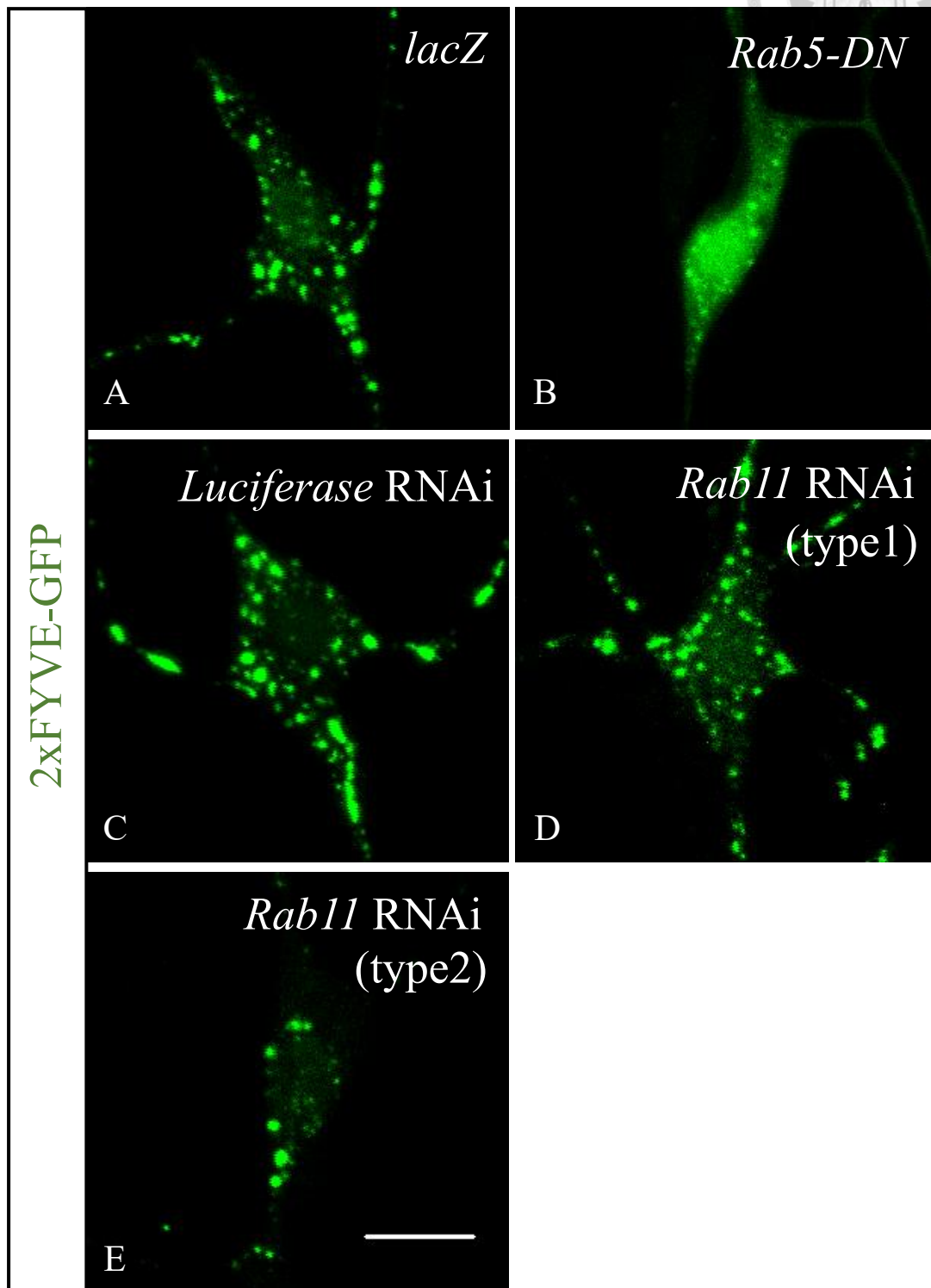


Figure 4. The three known Rab11 GEFs participate in regulation of dendrite morphogenesis in ddaC neurons..



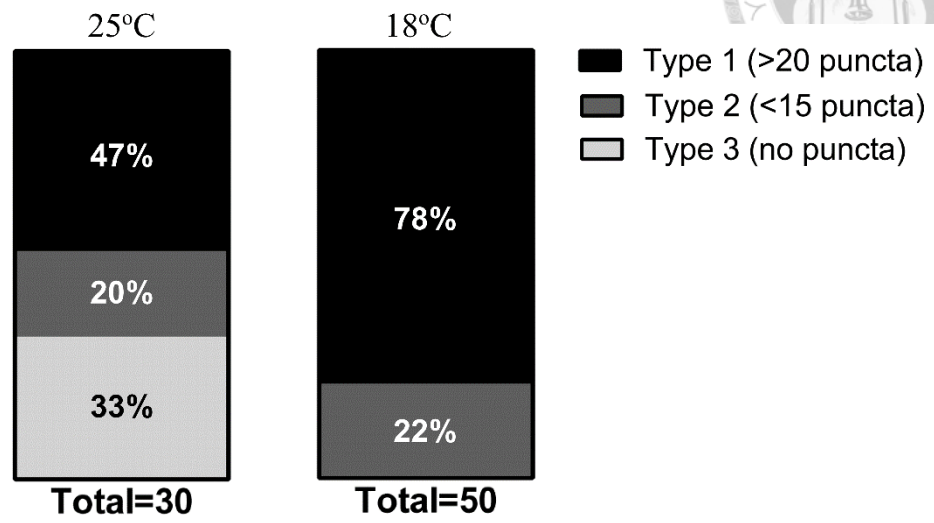
(A-F) The ddaC neurons were marked with *UAS-mCD8-GFP* driven by *ppk-Gal4*. The dendritic morphology was examined in control MARCM clones (A), *Crag^A* MARCM clones (B), heterozygous *pcs* mutant neurons (*pcs^{gs}/ +*) (C), homozygous *pcs* mutant neurons (*pcs^{gs}/ pcs^{gs}*) (D), neurons hemizygous for *brun* (*Df (brun)/ +*) (E), hemizygous *brun* mutant neurons (*brun^{Z0704}* or *brun^{Z3358}* over *Df(brun)*) (F, G), and neurons with transheterozygous mutant between *pcs* and *brun* (*pcs^{gs}/ Df (brun)*) (H). The number of neurons examined was as follows: for control MARCM clones, n=3; for *Crag^A* MARCM clones, n=11; for *pcs^{gs}/ +* and *Df (brun)/ +*, n=40; for *pcs^{gs}/ pcs^{gs}*, n=50; for *brun^{Z0704}/Df(brun)*, *brun^{Z3358}/Df(brun)* and *pcs^{gs}/Df(brun)*, n=30. Sholl analysis (I-K) and Strahler analysis (L-N) were performed to measure dendritic branching complexity in neurons with genotypes described in (A-H). The curve in Sholl analysis was plotted by average number of intersections. (O-Q) The percentage of area of dendritic coverage was calculated from dividing the dendritic area of mutant neurons by that of control ones (the bars on the far left in each panel). Scale bar, 50 μ m.

Figure 5

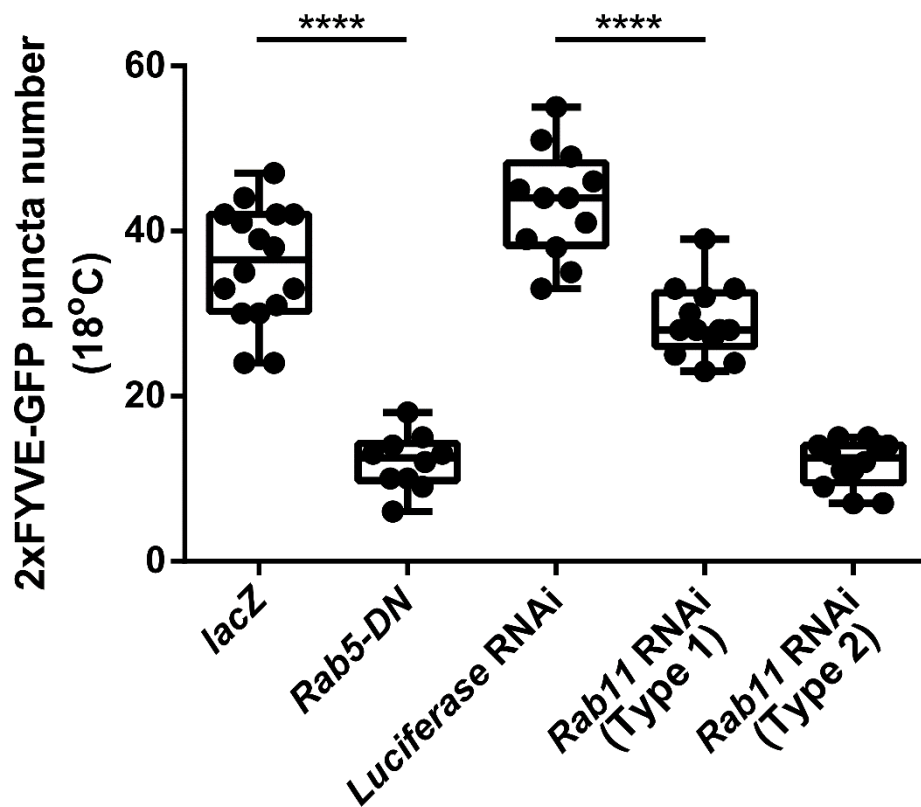




F 2xFYVE-GFP puncta signal in larval neurons with *Rab11*-RNAi



G



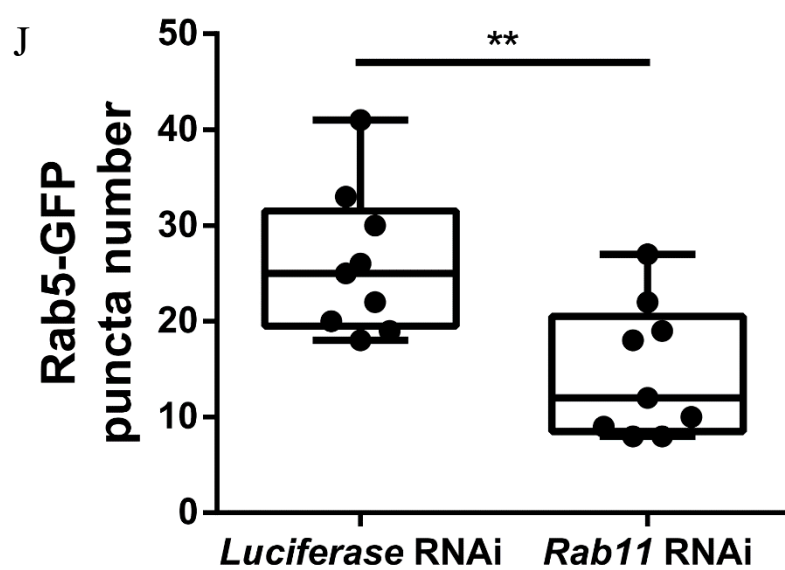
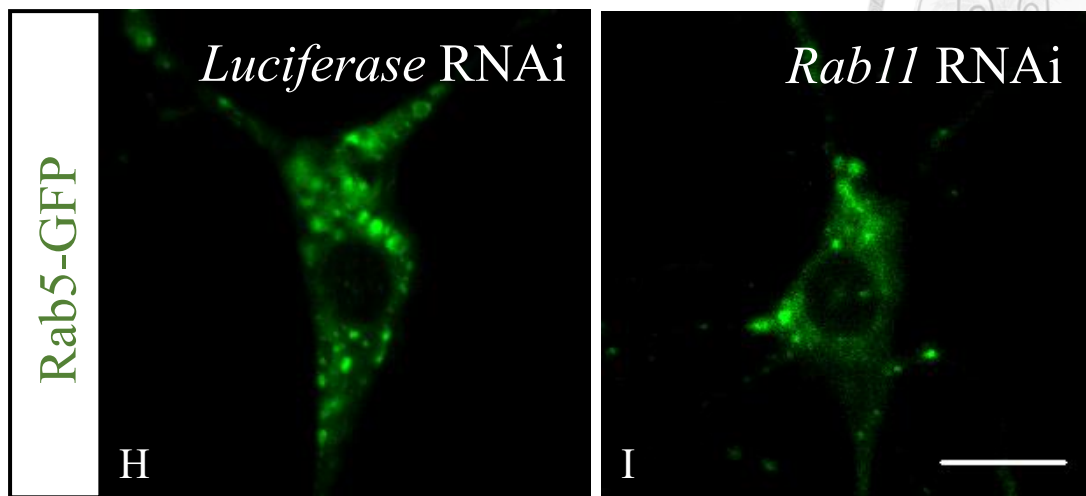


Figure 5. Endocytosis is impaired in *Rab11* mutant neurons.

(A-E) The *ppk-GAL4*-driven 2xFYVE-GFP in *lacZ*-expressing neurons (A), *Rab5-DN*-expressing neurons (B), neurons with *Luciferase* RNAi (C), and neurons with *Rab11* RNAi (D, E) in third instar larvae. (F) Quantification of 2xFYVE-GFP patterns in *Rab11* RNAi ddaC neurons in larvae reared at 25°C and 18°C. Total number stands for the number of neurons examined. (G) Quantitative analysis of 2xFYVE-GFP puncta number in larval ddaC neurons with genotypes described in panel A to E. The larvae were reared at 18°C. The number of neurons examined was as follows: for *lacZ*, n=16; for *Rab5-DN*, n=10; for *Luciferase* RNAi, n=12; for *Rab11* RNAi (normal), n=13; for *Rab11* RNAi (weak), n=13. (H, I) The distribution of *ppk-Gal4*-driven Rab5-GFP in third instar larval neurons with *Luciferase* RNAi (H) and larval neurons with *Rab11* RNAi (I). (J) Quantitative analysis of Rab5-GFP puncta number in larval ddaC neurons with *Luciferase* RNAi and *Rab11* RNAi. The number of neurons examined was as follows: for *Luciferase* RNAi, n=9; for *Rab11* RNAi, n=9. Scale bar, 10 μ m.

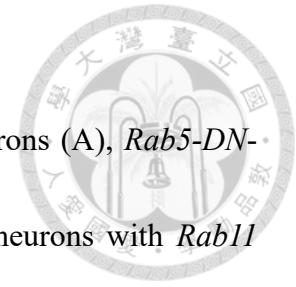
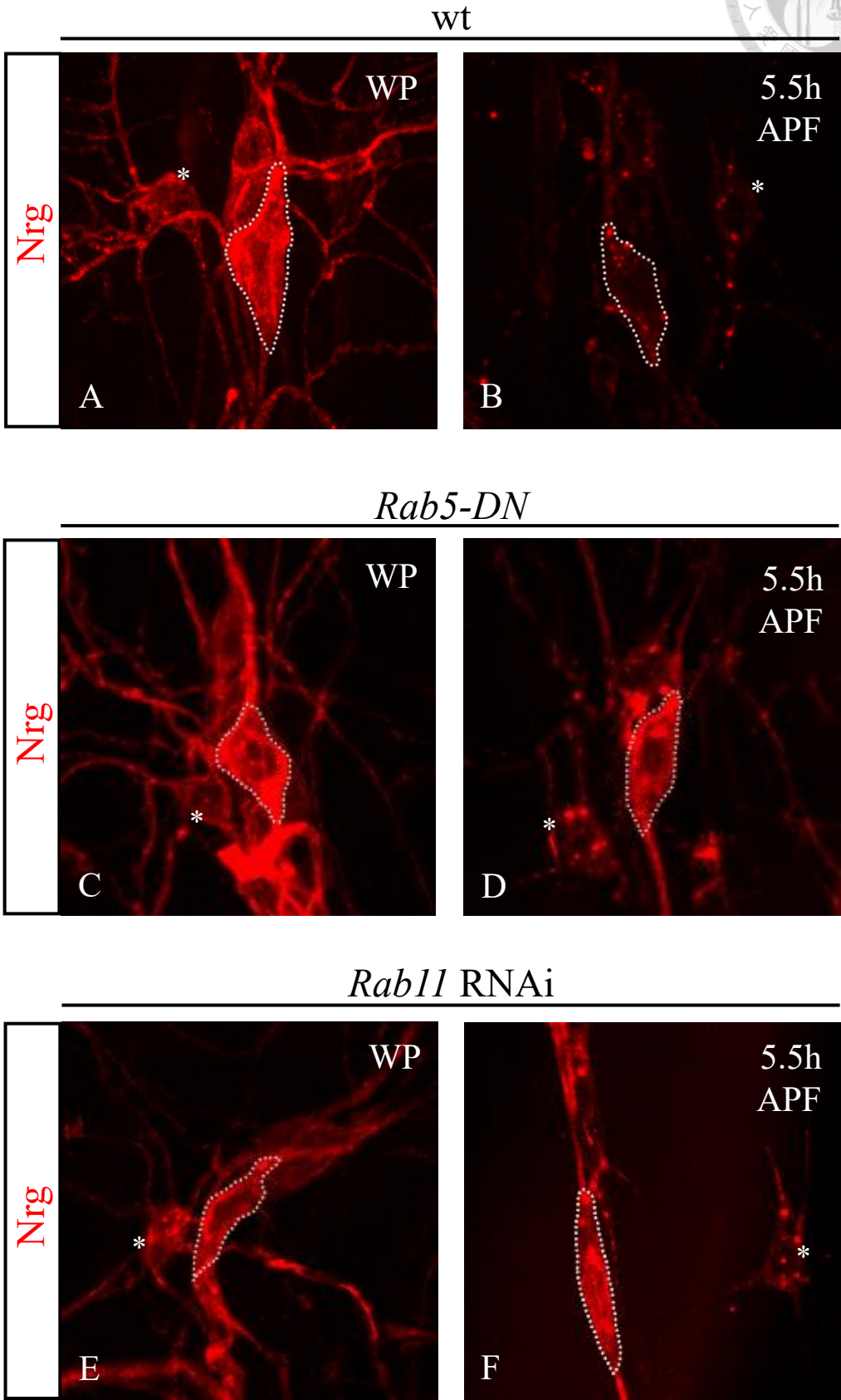


Figure 6



Rab11-DN

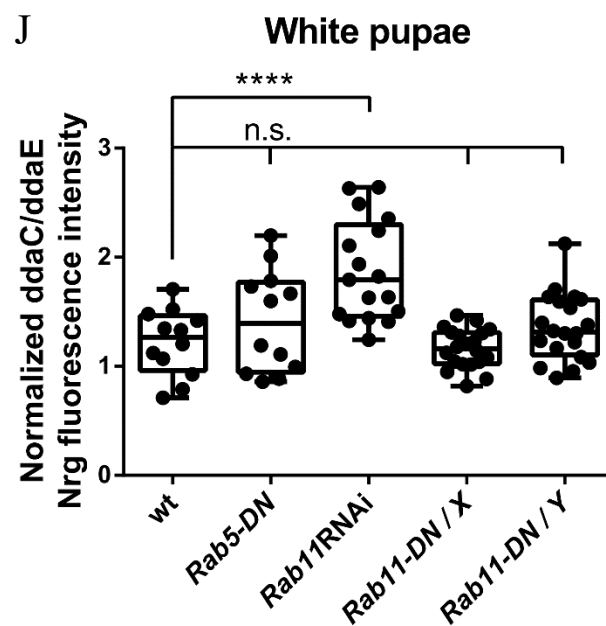
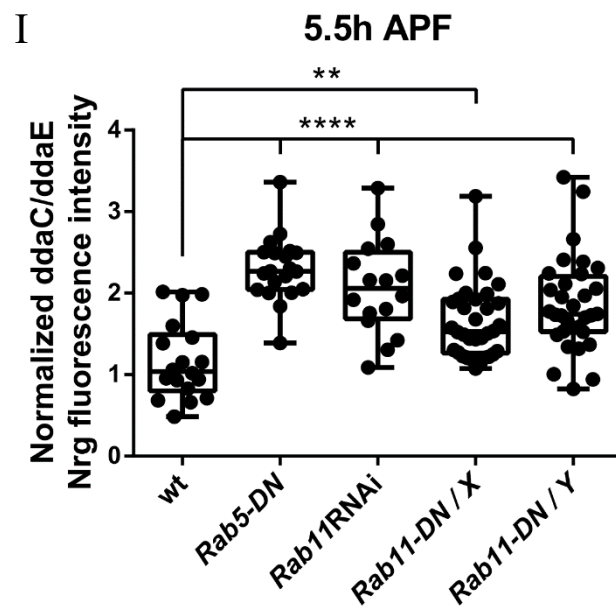
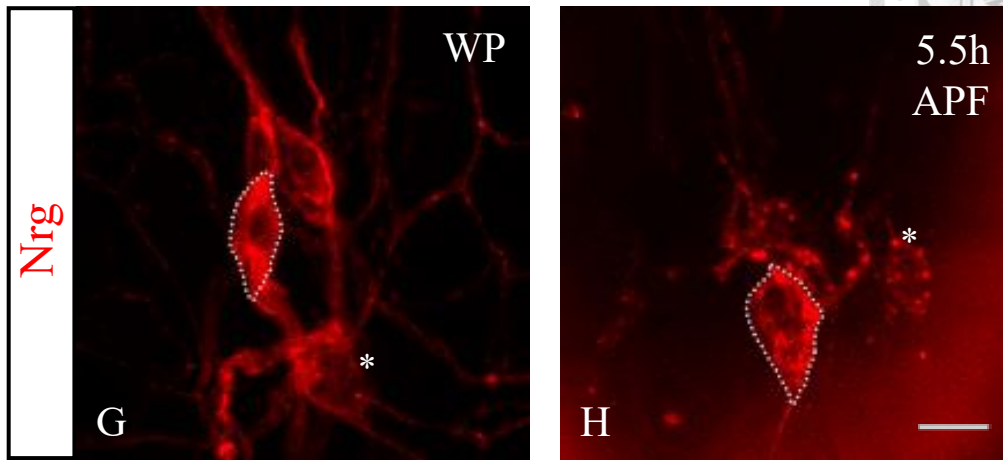
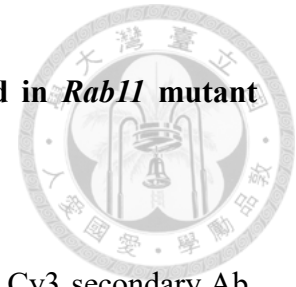


Figure 6. The Nrg-internalizing endocytic pathway is impaired in *Rab11* mutant neurons.



(A-H) Nrg was detected by staining with anti-Nrg primary Ab and Cy3 secondary Ab.

ddaC neurons were visualized by *GAL4*-driven *mCD8GFP* and their somas were labeled

with dashed line. ddaE neurons were marked by asterisks. (A, B) In wild-type neurons,

the membrane-localized Nrg during white pupal (WP) stage was internalized at 5.5h APF.

Nrg internalization was blocked in Rab5-DN-expressing neurons (C, D), *Rab11-dsRNAs*-

expressing neurons (E, F), and Rab11-DN-expressing neurons (G, H). (I, J) Quantitative

analysis of normalized ddaC/ddaE soma-surface-associated Nrg fluorescence signal

intensity in wild-type neurons, neurons with Rab5-DN expression, neurons with *Rab11*

RNAi, and neurons with one-fold (*Rab11-DN/+*) or two-fold (*Rab11-DN/Y*) expression

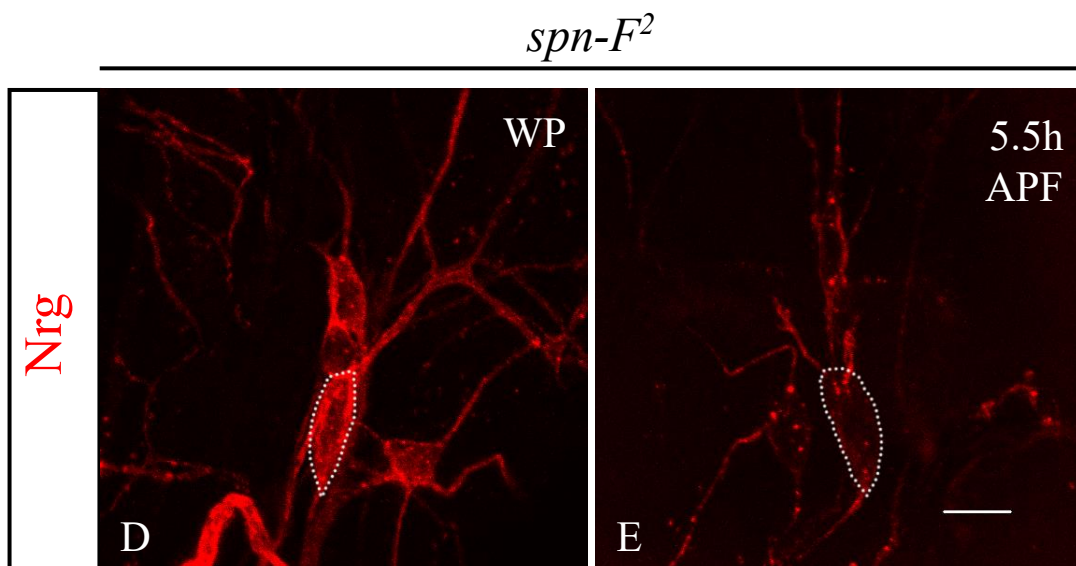
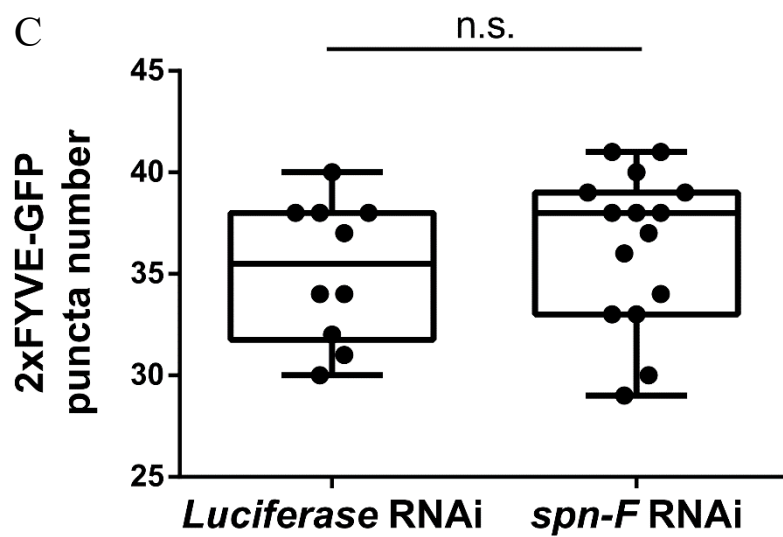
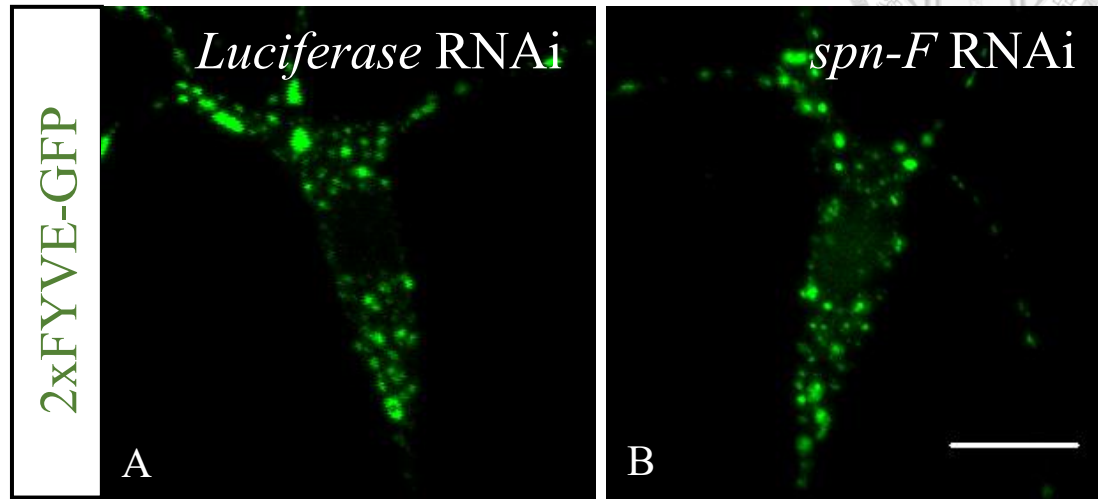
of Rab11-DN at 5.5h APF (I) and WP stage (J). Total number of neurons examined was

as follows: for wt, n=18 in (I), 12 in (J); for *Rab5-DN*, n=20 in (I), 12 in (J); for *Rab11*

RNAi, n=16 in (I), 17 in (J); for *Rab11-DN/+*, n=34 in (I), 20 in (J); for *Rab11-DN/Y*,

n=32 in (I), 20 in (J). Scale bar, 10 μ m.

Figure 7



F

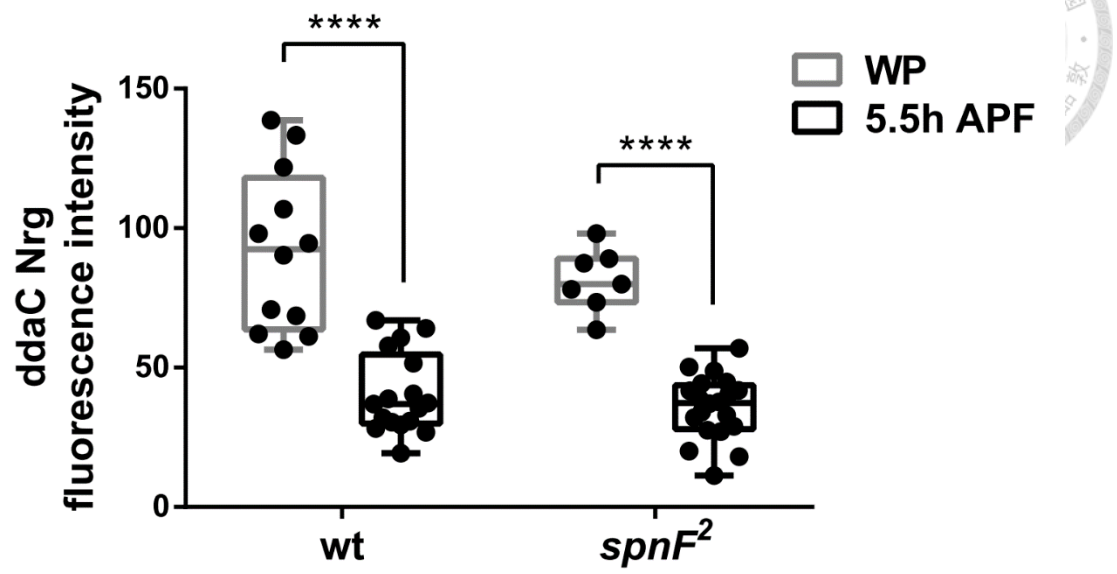
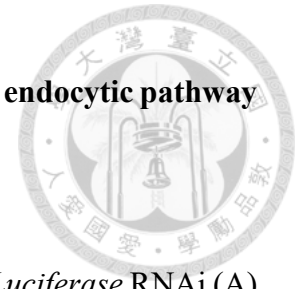


Figure 7. Spn-F is not required for maintaining Nrg-internalizing endocytic pathway in dendrite pruning of ddaC neurons.



(A, B) The *ppk-GAL4*-driven 2xFYVE-GFP pattern in neurons with *Luciferase* RNAi (A), and neurons with *spn-F* RNAi (B) in third instar larvae. (C) Quantitative analysis of 2xFYVE-GFP puncta number in larval ddaC neurons with genotypes described in panel A and B. The number of neurons examined was as follows: for *Luciferase* RNAi, n=10; for *Rab11* RNAi, n=15. (D, E) Nrg was detected by staining with anti-Nrg primary Ab and Cy3 secondary Ab. ddaC neurons were visualized by *GAL4*-driven *mCD8GFP* and their somas were labeled with dashed line. In *spn-F²* mutant neurons, the membrane-localized Nrg during white pupal (WP) stage was internalized at 5.5h APF. (F) Quantitative analysis of ddaC soma-surface-associated Nrg fluorescence signal intensity in wild-type neurons and *spn-F²* mutant neurons at WP stage and 5.5h APF. Total number of neurons examined was as follows: for wt, n=12 (WP)/17 (5.5h APF); for *spn-F²*, n=7 (WP)/20 (5.5h APF). Scale bar, 10 μ m.

Figure 8

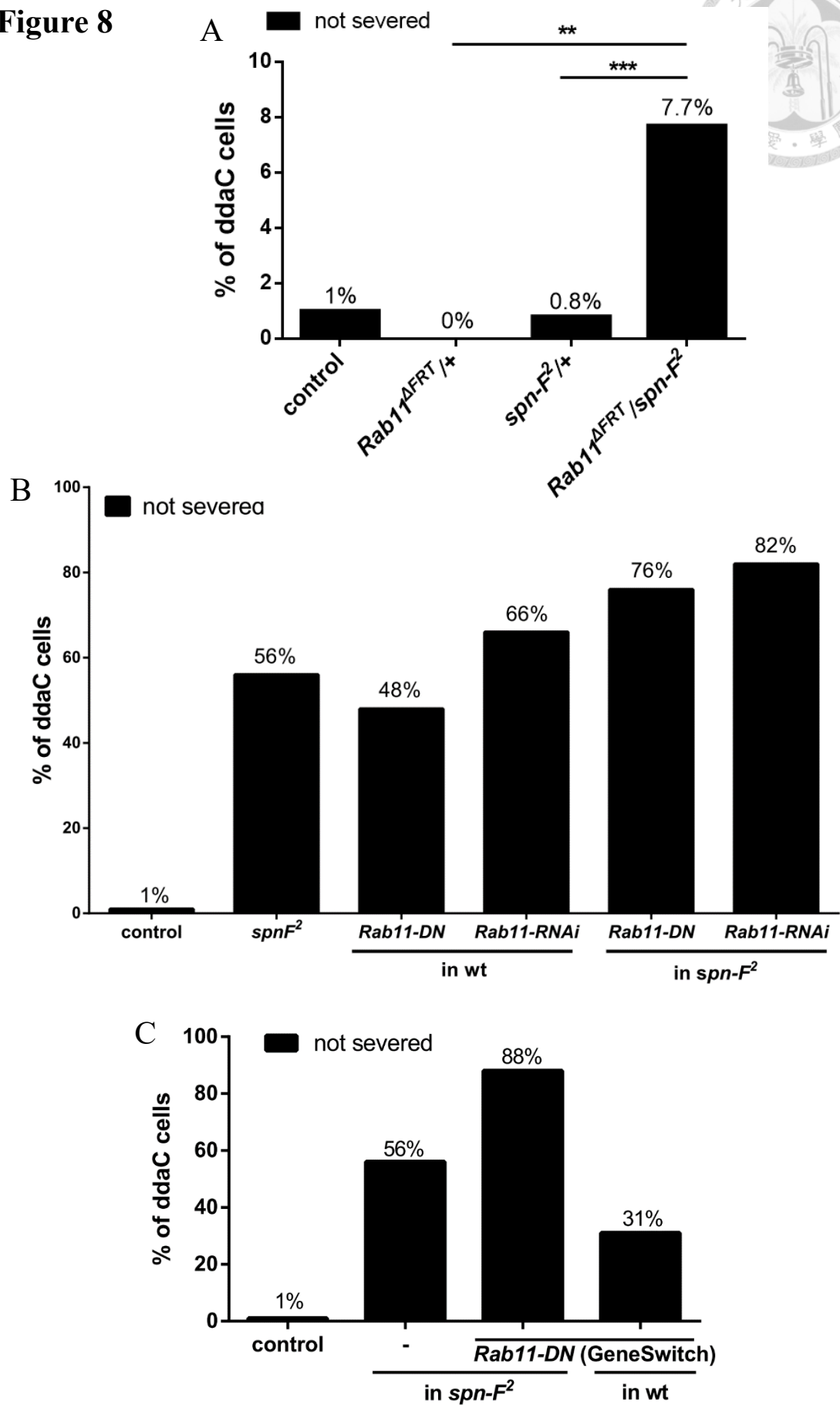
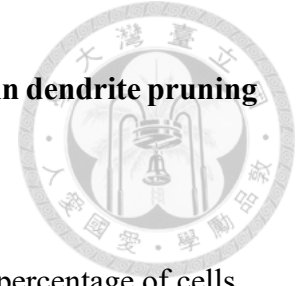


Figure 8. There is a genetic interaction between *Rab11* and *spn-F* in dendrite pruning of ddaC neurons.



(A-C) Quantitative analysis of pruning phenotypes at 16h APF. The percentage of cells was calculated by dividing the number of neurons with unsevered dendrites by total number of neurons examined in each genotype. (A) Pruning phenotypes were examined in control neurons (n=100), neurons of heterozygous mutants for either *Rab11* (*Rab11* ^{Δ FRT/+}, n=100) or *spn-F* (*spn-F*^{2/+}, n=250), and neurons of transheterozygous mutants for *Rab11* and *spn-F* (*Rab11* ^{Δ FRT/*spn-F*²}, n=220). (B) Pruning phenotypes were examined in control neurons (n=100), mutant neurons homozygous for *spn-F*² (n=100), *Rab11*-DN-expressing neurons (n=100), *Rab11*-dsRNA-expressing neurons (n=100), *Rab11*-DN-expressing neurons in *spn-F*² background (n=99), and *Rab11*-dsRNA-expressing neurons in *spn-F*² background (n=110). (C) Pruning phenotypes were examined in control neurons (n=100), mutant neurons homozygous for *spn-F*² (n=100), neurons with *Rab11*-DN expression induced at 96h AEL in *spn-F*² background (n=60), and neurons with *Rab11*-DN expression induced at 96h AEL (n=110).

Figure 9

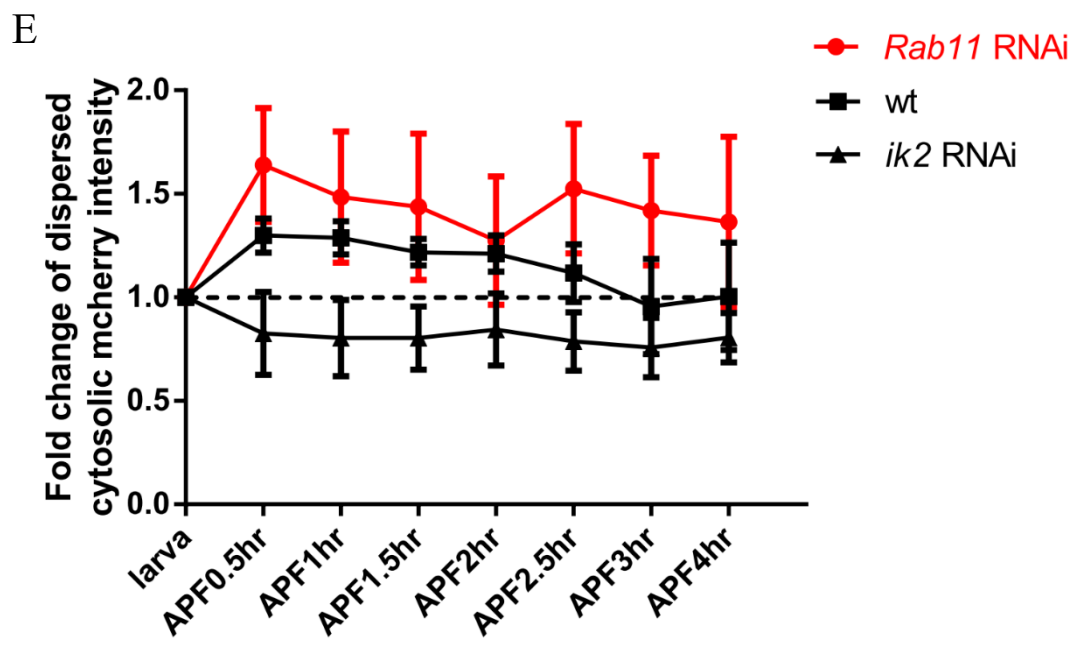
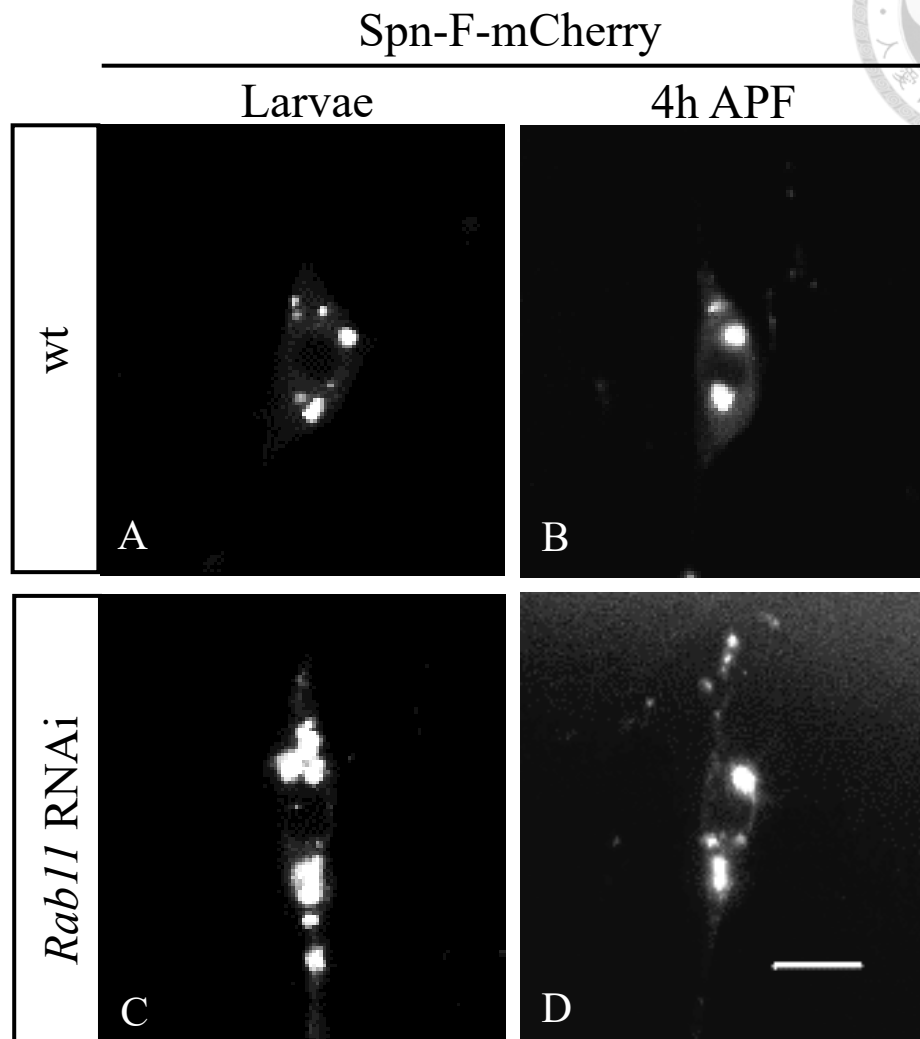


Figure 9. Ik2 kinase activation and Spn-F dispersion are normal in *Rab11* mutant neurons.

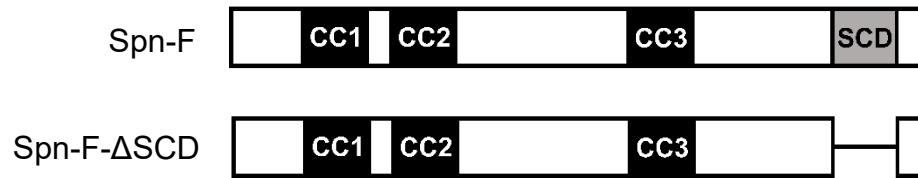


(A-D) Investigation of Spn-F puncta dispersion by expressing Spn-F-mCherry in both wild-type neurons and neurons with *Rab11* RNAi. (F) Time-lapse imaging was conducted in wild-type neurons and neurons with *Rab11* RNAi or *ik2* RNAi. The dispersed cytosolic mCherry fluorescent intensity was measured by averaging the non-punctate cytosolic signal intensity. The fold changes were determined by dividing the average cytosolic mCherry intensities in pupal neurons by those in the same larval neurons, which were assigned as 1. The number of neurons examined was as follows: for wild type and *Rab11* RNAi, n=5; for *ik2* RNAi, n=6. Scale bar, 10 μ m.

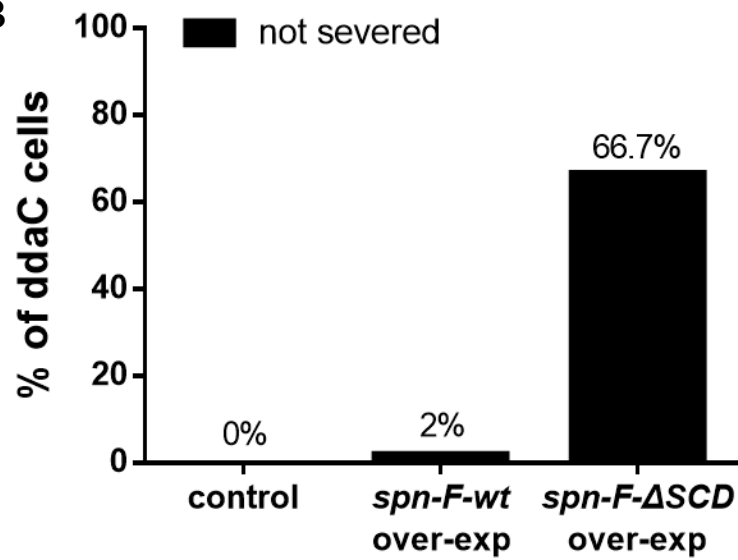
Figure 10



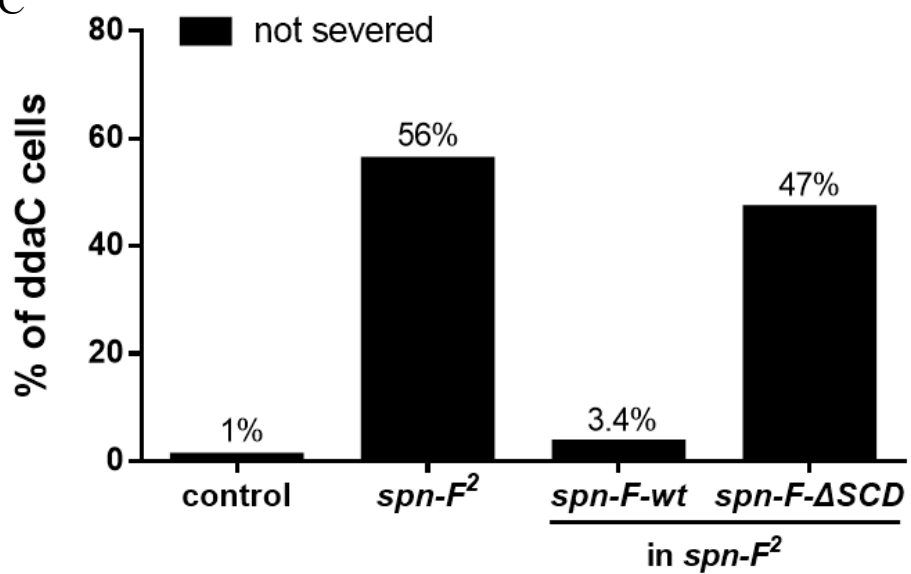
A



B



C



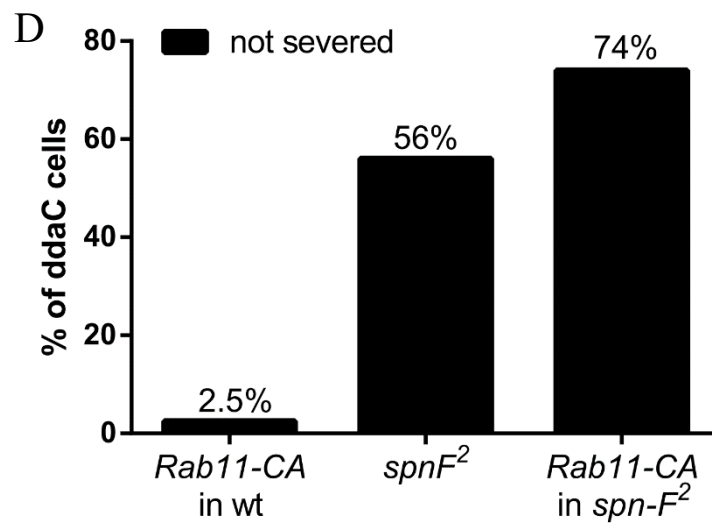


Figure 10. The Rab11-interacting domain of Spn-F is crucial for dendrite pruning in ddaC neurons.



(A) The schematic illustrates the wild-type and a SCD domain-trauncated (SpnF- Δ SCD)

Spn-F protein constructs. Spn-F have three coiled-coil domains (CC1, CC2 and CC3),

and a SpnF-conserved domain (SCD) at its C terminus. (B, C, D) Quantitative analysis of

pruning phenotypes at 16h APF in ddaC neurons. The percentage of cells was calculated

by dividing the number of neurons with unsevered dendrites by total number of neurons

examined in each genotype. The number of neurons examined was as follows: for control

in (B), n=60; for *spn-F-wt*, n=38; for *spn-F- Δ SCD*, n=90; for control in (C), n=100; for

spn-F², n = 110; for *spn-F²* rescued with wild-type *spn-F*, n = 88; for *spn-F²* rescued with

spn-F- Δ SCD, n = 100; for Rab11-CA over-expression, n=80; for Rab11-CA over-

expression in *spn-F²*, n=90. The experiments of wild-type *spn-F* over-expression, *spn-F²*

rescued with wild-type *spn-F*, and Rab11-CA over-expression were conducted by former

lab members.

Figure 11

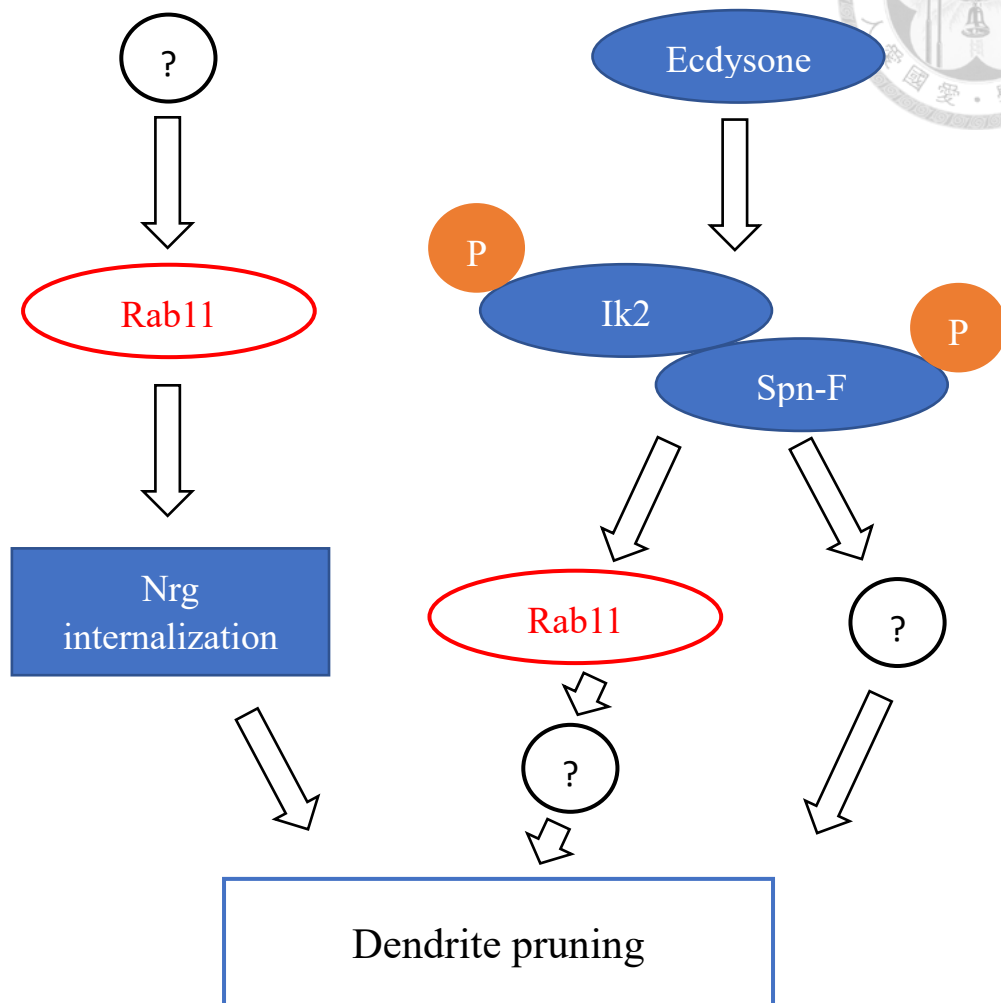
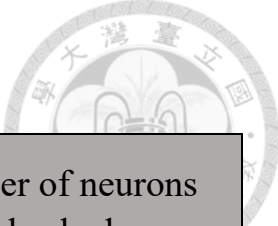


Figure 11. Proposed model of the roles of Rab11 in dendrite pruning in ddaC neurons.

Table 1



Genotype	Percentage of ddaC cells with unsevered dendrites	Number of neurons checked
<i>Crag^A</i> (MARCM)	0	6
<i>pcs^{gs}/pcs^{gs}</i>	0	110
<i>brun^{Z0704}/Df</i>	0	60
<i>brun^{Z3358}/Df</i>	0	70
<i>pcs^{gs}/Df</i>	0	30

Table 1. Dendrite pruning defects were not found in the ddaC neurons with mutation of the known Rab11 GEFs genes.